The relative importance of chlorine and bromine radicals in the oxidation of atmospheric mercury at Barrow, Alaska

Chelsea R. Stephens,[1] Paul B. Shepson,[1,2,3] Alexandra Steffen,[4] Jan W. Bottenheim,[4] Jin Liao,[5] L. Greg Huey,[5] Eric Apel,[6] Andy Weinheimer,[6] Samuel R. Hall,[6] Christopher Cantrell,[6] Barkley C. Sive,[7,8] D. J. Knapp,[6] D. D. Montzka,[6] and Rebecca S. Hornbrook[6]

Received 1 August 2011; revised 18 November 2011; accepted 18 December 2011; published 3 March 2012.

[1] Mercury is a toxic environmental contaminant originating from both natural and anthropogenic sources. Gaseous elemental mercury (GEM) is relatively long lived in the midlatitudes and can be transported long distances in the atmosphere. In the Polar Regions, mercury can have a much shorter lifetime and is known to experience episodic depletions following polar sunrise in concert with ozone depletion events. A series of photochemically initiated reactions involving halogen radicals is believed to be the primary pathway responsible for converting elemental mercury to oxidized forms of reactive gaseous mercury (RGM) that are subsequently deposited to snow and ice surfaces. Using field measurements from the Ocean-Atmosphere-Sea Ice-Snowpack (OASIS) 2009 field campaign of GEM, RGM, ozone, and a large suite of both inorganic halogen and volatile organic compounds, we calculated steady state Br and Cl atom concentrations and investigated the contribution of Br, BrO, Cl, ClO, O_3, and OH to the observed decay of GEM for five cases of apparent first-order decay. The results of this study indicate that Br and BrO are the dominant oxidizers for Arctic mercury depletion events, with Br having the greatest overall contribution to GEM decay. Ozone is likely the primary factor controlling the relative contribution of Br and BrO, as BrO is a product of the reaction of Br with ozone, and reaction with O_3 can be the largest Br atom sink. Cl was not found to be significant in any of the studied events; however, this result is highly dependent on the rate constant, for which there is a large range in the literature. Modeled 48 h back trajectories of the mercury depletion events studied here indicate significant time spent over sea ice–covered regions, where the concentration of halogen radicals is likely higher than those estimated using local-scale chemical mole fractions.

Citation: Stephens, C. R., et al. (2012), The relative importance of chlorine and bromine radicals in the oxidation of atmospheric mercury at Barrow, Alaska, *J. Geophys. Res.*, *117*, D00R11, doi:10.1029/2011JD016649.

1. Introduction

[2] Mercury is a naturally occurring heavy metal in the environment found globally in the air, oceans and soils. Anthropogenic sources add to the atmospheric burden of gaseous mercury through industrial activities such as fossil fuel burning, gold mining, cement production and waste incineration [*Pirrone et al.*, 2010; *Steffen et al.*, 2008]. Unlike other heavy metals, elemental mercury is a liquid metal with a high vapor pressure at ambient temperatures, resulting in the atmosphere serving as a significant route for both transport and chemical transformation [*Sommar et al.*, 2001].

[3] In the atmosphere, mercury exists primarily in its elemental state, Hg°. Gaseous elemental mercury (GEM) accounts for an estimated 95%–98% of airborne mercury, with oxidized forms, both gaseous and particulate, making up the rest [*Lindberg et al.*, 2002; *Steffen et al.*, 2008]. In midlatitudes, the residence time of GEM is estimated to be on the order of one year [*Schroeder et al.*, 1998; *Steffen et al.*, 2008], making it well distributed throughout the troposphere due to long-range transport, and effectively classifying it as a global pollutant. The northern hemispheric background of GEM is near 1.7–1.9 ng/m^3, with somewhat lower background

[1]Department of Chemistry, Purdue University, West Lafayette, Indiana, USA.
[2]Department of Earth and Atmospheric Sciences, Purdue University, West Lafayette, Indiana, USA.
[3]Purdue Climate Change Research Center, Purdue University, West Lafayette, Indiana, USA.
[4]Air Quality Research Division, Environment Canada, Toronto, Ontario, Canada.
[5]School of Earth and Atmospheric Sciences, Georgia Institute of Technology, Atlanta, Georgia, USA.
[6]National Center for Atmospheric Research, Boulder, Colorado, USA.
[7]Institute for the Study of Earth, Oceans, and Space, University of New Hampshire, Durham, New Hampshire, USA.
[8]Now at Department of Chemistry, Appalachian State University, Boone, North Carolina, USA.

0148-0227/12/2011JD016649

values reported for the southern hemisphere and the poles [*Nguyen et al.*, 2009; *Slemr et al.*, 2003; *Steffen et al.*, 2008]. The dry deposition and wet scavenging rates for RGM and particulate mercury species are about an order of magnitude higher than that of GEM [*Lindberg et al.*, 2002], and thus they are expected to have a rather short lifetime in the atmosphere, in contrast to GEM, which can be transported far from sources and impact remote ecosystems such as the polar regions. Depending on its chemical form, mercury is also one of the most toxic elements found in nature [*Ariya et al.*, 2002], and has been identified by the Arctic Monitoring and Assessment Programme (AMAP) as a "priority pollutant" in the Arctic of primary concern [*AMAP*, 2011].

[4] Current knowledge regarding the biogeochemical mercury cycle indicates numerous sources, but few known sinks. The global-scale chemical sinks for GEM have been believed to be OH and O_3; however, this removal mechanism is relatively slow [*Holmes et al.*, 2006]. In the mid 1990s, it was recognized that in the high Arctic GEM experiences precipitous drops from background levels to less than 0.1 ng/m^3 for time scales of a few hours to several days [*Lu et al.*, 2001], in concert with ozone depletion events (ODEs) in the high Arctic [*Schroeder et al.*, 1998]. This behavior was unexpected for a pollutant with a long atmospheric lifetime in midlatitude regions, and it was suggested that halogen photochemistry unique to the polar regions was responsible for the observed GEM depletions [*Lu et al.*, 2001; *Schroeder et al.*, 1998], in a similar manner as that which occurs for tropospheric ozone [*Simpson et al.*, 2007b].

[5] It is now known that GEM is oxidized to reactive gaseous inorganic mercury (RGM) species, likely consisting of Hg^{II} compounds, that can subsequently be deposited to snow and ice surfaces during these atmospheric mercury depletion events (AMDEs). Oxidized mercury compounds can also be scavenged by aerosols to form particulate mercury (PHg) [*Steffen et al.*, 2008]. A fraction of the deposited RGM is photoreduced back to elemental mercury and evaded from the surface [*Brooks et al.*, 2006; *Lalonde et al.*, 2002; *Lindberg et al.*, 2002; *Poulain et al.*, 2004]. Currently, there is no analytical method in the published literature capable of speciating RGM, and it is thus operationally defined [*Steffen et al.*, 2008] and measured by collection on a KCl-coated denuder (known to collect $HgCl_2$ efficiently) followed by thermal reduction and detection as elemental Hg. As a result, the chemical composition of RGM (and particulate Hg) remains undetermined. Halogen-containing radicals are speculated to be the primary oxidizers of GEM in this environment, initiated by the heterogeneous reaction of ozone with sea salt derived chloride or bromide [*Foster et al.*, 2001; *Impey et al.*, 1997b; *Oum et al.*, 1998a]. RGM production has been observed to be photochemical in nature, with a clear diurnal cycle [*Lindberg et al.*, 2002], lending support to the hypothesis that photochemically generated oxidants are depleting GEM and producing RGM. A more recent modeling study on the global mercury cycle has also suggested that Br is a significant oxidant in the atmosphere for Hg° at middle and low latitudes as well [*Holmes et al.*, 2006, 2010].

[6] The source of the halogen-atom precursors, such as Br_2, Cl_2, HOBr, and HOCl, is believed to be the hypersaline brine surfaces on young sea ice, frost flowers, and surface hoar adjacent to refreezing leads [*Douglas et al.*, 2005; *Kaleschke et al.*, 2004; *Simpson et al.*, 2007a], and from saline snowpacks [*Foster et al.*, 2001]. The primary pathway for ozone destruction has been recognized to be reaction with bromine atoms resulting in the now well-known "bromine explosion." In this mechanism, gas-phase Br reacts with O_3 to produce O_2 and BrO, followed by heterogeneous surface reactions that result in the autocatalytic release of additional reactive Br [*Platt and Hönninger*, 2003]. Consistent with this proposed mechanism, ground-based and satellite differential optical absorption spectroscopy (DOAS) measurements in the Arctic region have shown up to 41 ppt BrO during periods of active ozone depletions [*Hausmann and Platt*, 1994; *Liao et al.*, 2011; *Pöhler et al.*, 2010; *Richter et al.*, 1998]. Surface DOAS measurements have corroborated this, with BrO generally observed to be negatively correlated with GEM in polar spring [*Brooks et al.*, 2006; *Ferrari et al.*, 2008]. Possible oxidation pathways for GEM thus include reactions (R1) and (R2).

$$\mathrm{Br} + \mathrm{Hg}^{\circ} \rightarrow \text{products} \quad (R1)$$

$$\mathrm{BrO} + \mathrm{Hg}^{\circ} \rightarrow \text{products}. \quad (R2)$$

Field measurements have been unable to differentiate between Br and BrO as oxidants of GEM, however, because direct measurements of Br have not been achieved.

[7] The presence of aggressive chlorine atom chemistry in the Arctic has been well recognized [*Ariya et al.*, 1998; *Boudries and Bottenheim*, 2000; *Jobson et al.*, 1994; *Keil and Shepson*, 2006; *Muthuramu et al.*, 1994; *Ramacher et al.*, 1999; *Rudolph et al.*, 1999]. Chlorine atoms can efficiently oxidize a wide range of volatile organic compounds. In the Arctic regions where water vapor and thus, the hydroxyl radical, are in low concentrations, chlorine atoms can serve as the primary sink for many of these species. Direct measurements of inorganic chlorine species other than chloride [*Pszenny et al.*, 1993] are scarce, primarily due to a lack of suitable analytical techniques. *Impey et al.* [1997b] measured photolyzable chlorine (Cl_2 and HOCl) at Alert, Canada at concentrations up to 100 ppt. The ClO molecule (a product of chlorine atom reaction with ozone) has also been measured, though with high uncertainty, at levels between 3 and 20 ppt at Ny-Ålesund, Spitsbergen [*Perner et al.*, 1999; *Tuckermann et al.*, 1997]. Similar to the bromine radicals, Cl and ClO could serve as oxidizers of GEM [*Ariya et al.*, 2002; *Skov et al.*, 2004] as shown in reactions (R3) and (R4).

$$\mathrm{Cl} + \mathrm{Hg}^{\circ} \rightarrow \text{products} \quad (R3)$$

$$\mathrm{ClO} + \mathrm{Hg}^{\circ} \rightarrow \text{products} \quad (R4)$$

The potential contribution of chlorine radicals to the springtime depletion of mercury has not been elucidated due to the absence of chlorine radical measurements in the Arctic.

[8] Numerous laboratory investigations have been aimed at studying the kinetics of GEM oxidation with several oxygenated and halogenated species, and the results of these works are summarized in Table 1. The relatively slow rate of the gas-phase reaction of GEM with ozone [*Hall*, 1995; *Pal and Ariya*, 2004a; *Spicer et al.*, 2002] indicates an

Table 1. Reported Second-Order Rate Constants From Previous Work for the Reactions of Hg° With Several Oxygenated and Halogenated Oxidants

Oxidant	k (cm^3 $molecule^{-1}$ s^{-1})	Reference[a]
O_3	$3\ (\pm 2) \times 10^{-20}$	*Hall* [1995]
	9×10^{-19}	*Spicer et al.* [2002]
	$7.5\ (\pm 0.9) \times 10^{-19}$	*Pal and Ariya* [2004b]
OH	$8.7\ (\pm 2.8) \times 10^{-14}$	*Sommar et al.* [2001]
	$9.0\ (\pm 1.3) \times 10^{-14}$	*Pal and Ariya* [2004a]
Br_2	$0.9\ (\pm 0.2) \times 10^{-16}$	*Ariya et al.* [2002]
	no reaction detected	*Spicer et al.* [2002]
Cl_2	$1.0–2.6 \times 10^{-18}$	*Ariya et al.* [2002]
	5×10^{-17}	*Spicer et al.* [2002]
Br	$3.2\ (\pm 0.3) \times 10^{-12}$	*Ariya et al.* [2002]
	9.7×10^{-13}	*Spicer et al.* [2002]
	$6.1\ (\pm 2.2) \times 10^{-13}$	*Donohoue et al.* [2006]
Cl	$1.5–5.0 \times 10^{-11}$	*Horne et al.* [1968]
	$1.0\ (\pm 0.2) \times 10^{-11}$	*Ariya et al.* [2002]
	6.4×10^{-11}	*Spicer et al.* [2002]
	$1.0\ (\pm 0.7) \times 10^{-12}$	*Donohoue et al.* [2005]
BrO	3.0×10^{-14}	*Spicer et al.* [2002]
	$1.0 \times 10^{-13}–1.0 \times 10^{-15}$	*Raofie and Ariya* [2003]
ClO	3.6×10^{-17}	*Spicer et al.* [2002]

[a]Experiments by *Donohoue et al.* [2005, 2006] performed in N_2 bath gas; second-order rate constant calculated for 248 K from reported Arrhenius expression. Experiment by *Horne et al.* [1968] performed in Ar and CF_3Cl bath gas. Experiment by *Ariya et al.* [2002] performed in N_2 bath gas.

atmospheric lifetime of GEM of between 20 days to over a year at 30 ppb ozone. Experimental evidence suggests, however, that heterogeneous reactions enhanced by surfaces or aerosols is the most probable mechanism for Hg° oxidation by O_3, rather than gas-phase reaction [*Subir et al.*, 2011]. Indeed, product studies determined that solid mercuric oxide, $HgO_{(s)}$, is the dominant product and $HgO_{(g)}$ was not observed [*Pal and Ariya*, 2004a]. Reported rate coefficient values for the reaction of GEM with OH [*Pal and Ariya*, 2004b; *Sommar et al.*, 2001] indicate an average GEM lifetime at global mean OH concentrations ($\sim 1 \times 10^6$ molecules/cm^3 [*Montzka et al.*, 2000]) of 4–7 months. Moreover, the lifetime of GEM against oxidation by H_2O_2 is on the order of 1.5–3.7 years [*Tokos et al.*, 1998], making this pathway considerably less important. It should be noted that these lifetime estimates are based only on the oxidation reactions to Hg^{II}, and do not take into account reduction back to GEM. These studies indicate that consumption by the prominent atmospheric oxidants is unable to produce the fast destruction of GEM observed during AMDEs in the Arctic regions.

[9] Oxidation of elemental mercury by halogenated radicals is a likely possibility given the close correlation of AMDEs and ODEs and the observed photochemical behavior of RGM production. *Ariya et al.* [2002] used a relative rate approach to determine the rate constant for reaction of Cl atoms with GEM, and reported a value for k_3 of $1.0\ (\pm 0.2) \times 10^{-11}$ cm^3 $molecule^{-1}$ s^{-1}, close to the 1.5×10^{-11} derived by *Horne et al.* [1968]. The same authors determined the rate constant for GEM + Br (k_1) to be $3.2\ (\pm 0.3) \times 10^{-12}$ cm^3 $molecule^{-1}$ s^{-1}. More recently, *Donohoue et al.* [2006] measured an effective second-order rate constant for k_1 of $6.1\ (\pm 2.2) \times 10^{-13}$ cm^3 $molecule^{-1}$ s^{-1} (calculated for 248 K) by an absolute method using pulsed laser induced fluorescence. The effective second-order rate constant for GEM + Cl was determined to be $1.0\ (\pm 0.7) \times 10^{-12}$ cm^3 $molecule^{-1}$ s^{-1} in N_2 bath gas [*Donohoue et al.*, 2005] by the same method. In the case of Cl atom reaction, the authors indicated an apparent rate coefficient 4 times faster when performed in air, presumably due to enhancement from reaction with radicals such as ClO and ClO_2. This observation, as well as the inconsistent results obtained by *Ariya et al.* [2002] using different reference compounds, and their observations of the impacts of the presence of air, casts doubt on the use of the relative rate method for this particular reaction. *Raofie and Ariya* [2003] estimated a range for k_2 (GEM + BrO) between 1.0×10^{-13} and 1.0×10^{-15} cm^3 $molecule^{-1}$ s^{-1}. *Spicer et al.* [2002] reported a value for k_2 of 3.0×10^{-14}. The only known study of reaction (R4) resulted in a rate constant of $k_4 = 3.6 \times 10^{-17}$ cm^3 $molecule^{-1}$ s^{-1}, significantly slower than for the other halogen radicals [*Spicer et al.*, 2002]. The slow reaction kinetics observed in reactions of GEM with the molecular halogens, Cl_2 and Br_2, make these species unlikely sinks for GEM in the atmosphere [*Ariya et al.*, 2002; *Spicer et al.*, 2002].

[10] A number of theoretical studies have been performed to investigate the thermodynamics and energetics of gas phase Hg° oxidation. The HgO molecule is predicted to be unstable, making O_3 oxidation of Hg° through O-atom transfer unfavorable [*Castro et al.*, 2009; *Tossell*, 2003], and it is very unlikely that oxidation of Hg° by O_3 proceeds via homogeneous gas-phase reaction [*Subir et al.*, 2011; *Hynes et al.*, 2009]. Similarly, the reaction of GEM with BrO is predicted to be endergonic if it proceeds via O-atom transfer. *Khalizov et al.* [2003] drew a similar conclusion, stating that it is unlikely to form HgO directly from BrO oxidation. An ab initio study by *Balabanov and Peterson* [2003] found that while the O-atom transfer reaction (i.e., Hg° + BrO → HgO + Br) is endothermic, the insertion reaction is exothermic (i.e., Hg° + BrO → BrHgO). The addition of a Br atom [*Tossell*, 2003] or Cl atom [*Maron et al.*, 2008] to Hg° is predicted to be exergonic, with the addition of a second halogen atom even more favorable than the first, at a rate constant close to the high-pressure limit [*Goodsite et al.*, 2004]. $HgBr_2$ and $HgCl_2$ are more stable thermally than HgBr and HgCl, and thus are more likely candidates for RGM. Product studies by *Ariya et al.* [2002] confirm that $HgCl_2$ and $HgBr_2$ are the dominant products from reaction of mercury with the respective halogen atoms.

[11] Although the Cl-atom initiated reaction rate constant is larger than for Br or BrO reaction with GEM, many studies have concluded that Br is the most probable driver of Arctic AMDEs [*Ariya et al.*, 2002, 2004; *Brooks et al.*, 2006; *Calvert and Lindberg*, 2003, 2004; *Goodsite et al.*, 2004; *Skov et al.*, 2004], due to the larger estimated Br atom atmospheric abundances [*Jobson et al.*, 1994; *Keil and Shepson*, 2006]. As there is currently no analytical technique able to measure Cl and Br atoms directly, several studies have calculated time-integrated concentrations based on rates of hydrocarbon decays [*Ariya et al.*, 1998; *Boudries and Bottenheim*, 2000; *Jobson et al.*, 1994; *Ramacher et al.*, 1999; *Rudolph et al.*, 1999] and an estimated reaction time of 1–20 days. The average bromine-atom concentration derived from this method is approximately 1×10^7 molecules/cm^3, while the average chlorine-atom concentration is about 1×10^4 molecules/cm^3. Therefore, using this method, [Br]/[Cl] ≈ 10^3. However, time-integrated estimates calculate [Br] and [Cl] averaged over the lifetime of the VOCs, and do not

reflect fluctuations in [Br] and [Cl], or the near-surface concentrations. The [Br]/[Cl] ratio can thus increase or decrease in response to changing chemical or meteorological conditions. *Keil and Shepson* [2006] found that [Br]/[Cl] ranges from 80 to 990 during partial ODEs, thus on the low end of this ratio (i.e., when [Cl] is relatively high or [Br] is relatively low), Cl atoms might be able to compete in GEM depletion. It has also recently been shown that Cl_2 can be produced by unknown chemistry involving O_3 (J. Liao et al., Unexpected high levels of molecular chlorine detected in the Arctic and its impact on tropospheric ozone depletion, manuscript in preparation, 2012). Since O_3 is the main sink for Br atoms, when O_3 is high, Cl atom chemistry can be important, and when O_3 is depleted, Br atom chemistry becomes relatively more important.

[12] In this study, we aim to investigate the quantitative contribution of the halogen radicals Br, BrO, Cl, and ClO to the depletion of GEM in the Arctic using data from the OASIS 2009 field campaign in Barrow, Alaska. During OASIS 2009, in situ measurements of GEM, RGM, particulate Hg (PHg), O_3, OH, and numerous VOCs and inorganic halogen species, including Cl_2, Br_2, BrO and ClO were conducted. These data were used to calculate time-varying estimates of Br and Cl atom concentrations using a steady state approximation. We report here the relative contribution of possible gas-phase oxidation pathways for AMDEs observed during the OASIS campaign at Barrow, Alaska.

2. Experimental Setup

[13] Data used in the study were collected during the Ocean-Atmosphere-Sea Ice-Snowpack (OASIS; www.oasishome.net) 2009 field campaign that took place from February to April of 2009 in Barrow, Alaska. Measurements of all species, with the exception of ClO, were conducted from portable trailers near the Barrow Arctic Research Center (BARC) building (71°19′29″N, 156°40′4″W), located 0.6 km southeast of the Chukchi Sea and 4 km northeast of the town of Barrow. ClO measurements were conducted at the KBRW radio tower (71°15′15″N, 156°30′27″W) located 10 km southeast of the Chukchi Sea. Instrumental methods for all measurements are described in detail elsewhere [*Liao et al.*, 2011; *Mauldin et al.*, 1999; *Ridley et al.*, 1992; *Schroeder and Munthe*, 1998; *Shetter and Müller*, 1999]. For those species on which this analysis most heavily relies, a brief overview is included here.

[14] Three lines on a tower, with sample heights of 0.6, 1.8, and 5.4 m, were used to sample O_3, with dwell times of 10 min at each of the 3 heights. O_3 was measured using the chemiluminescence technique with a 1 s detection limit of 0.02 parts per billion by volume (ppbv), as described by *Ridley et al.* [1992]. Data were acquired at a 1 Hz sample rate.

[15] Gaseous elemental mercury (GEM), reactive gaseous mercury (RGM) and particle associated mercury (PHg) were determined during the OASIS 2009 campaign using automated Tekran 2537A, Tekran 1130, and Tekran 1135 instruments, respectively. GEM was measured using a Tekran 2537A mercury vapor analyzer. This method has been summarized by *Steffen et al.* [2008]. The Tekran 1130 and 1135 systems are front end modules that connect to the Tekran 2537A to collect RGM and PHg, respectively, and convert oxidized mercury forms to elemental mercury by pyrolysis. Because calibration with authentic RGM and PHg standards is currently not possible at this time, these two species must be considered, at best, operationally defined atmospheric species as presented in this publication, and are only used as relative concentrations.

[16] BrO, Br_2, BrCl, HOBr, and Cl_2 were detected by chemical ionization mass spectrometry (CIMS). The CIMS was actively calibrated in the field using permeation sources of Br_2 and Cl_2. The CIMS instrument used during the OASIS campaign and the calibration procedures for BrO, Br_2, and Cl_2 are described in detail by *Liao et al.* [2011]. BrCl levels were calculated assuming a relative sensitivity of the CIMS to Br_2 and BrCl that is identical to that reported by *Neuman et al.* [2010]. HOBr levels were calculated relative to Br_2 levels. The relative sensitivity of HOBr to Br_2 was measured in the laboratory after the campaign. Gas-phase HOBr was synthesized in the laboratory by liberating HOBr formed in solution by the hydrolysis of Br_2 as shown in reaction (R5).

$$\text{(R5)} \qquad Br_2 + H_2O \rightarrow HOBr + Br^- + H^+.$$

[17] The hydrolysis reaction is performed by flowing humidified N_2 and Br_2 in N_2 over glass beads coated with $AgNO_3$ as described by *Neuman et al.* [2010]. The concentration of HOBr was determined by conversion back to Br_2 via reaction with solid sodium bromide and subsequent measurement of Br_2. The uncertainty of the Br_2, Cl_2, and BrCl measurements is estimated to be ±25%. The uncertainty of the HOBr and BrO measurements is estimated to be ±35%.

[18] In situ measurements of ClO were performed using a flowing chemical reaction method that draws ambient air through a flow tube and quantitatively converts the reactive radical species to a stable halogenated acetone product using a reactive alkene as a halogen atom trap, similar to the method described by *Impey et al.* [1997a]. 1,1,1-trifluoropropene, a compound that is not present in ambient air, was used to scavenge the halogen atoms. The product, 1-chloro-3,3,3-trifluoroacetone, is then separated and detected using a gas chromatograph with electron capture detection. Calibrations were performed both prior to deployment and weekly in the field using solutions of 1-chloro-3,3,3-trifluoroacetone in diethyl ether. Field blanks were performed weekly by turning off the flow of 1,1,1-trifluoropropene to the flow tube. The limit of detection, calculated as three times the standard deviation of the blank, was 0.65 pptv. The propagated uncertainty of the measurements is calculated to be ±15%, taking into account loss of the radical on the reaction walls, reaction time and product yield of the chemical reaction, loss of the reaction product on the sample line, error in the calibration, and variability of the blanks. However, there could be unknown systematic errors that would lead to a larger uncertainty. Given the small value for k_4 and the low ambient ClO concentrations observed, the conclusions discussed below will not be significantly impacted if this were the case.

[19] The Trace Organic Gas Analyzer (TOGA) using fast online gas chromatography coupled with mass spectrometry (GC-MS) was used to measure up to 30 different volatile organic compounds (VOCs) during OASIS as described by *Apel et al.* [2010]. The VOCs observed by TOGA during OASIS include NMHC (C_4 and C_5 alkanes, isoprene, benzene,

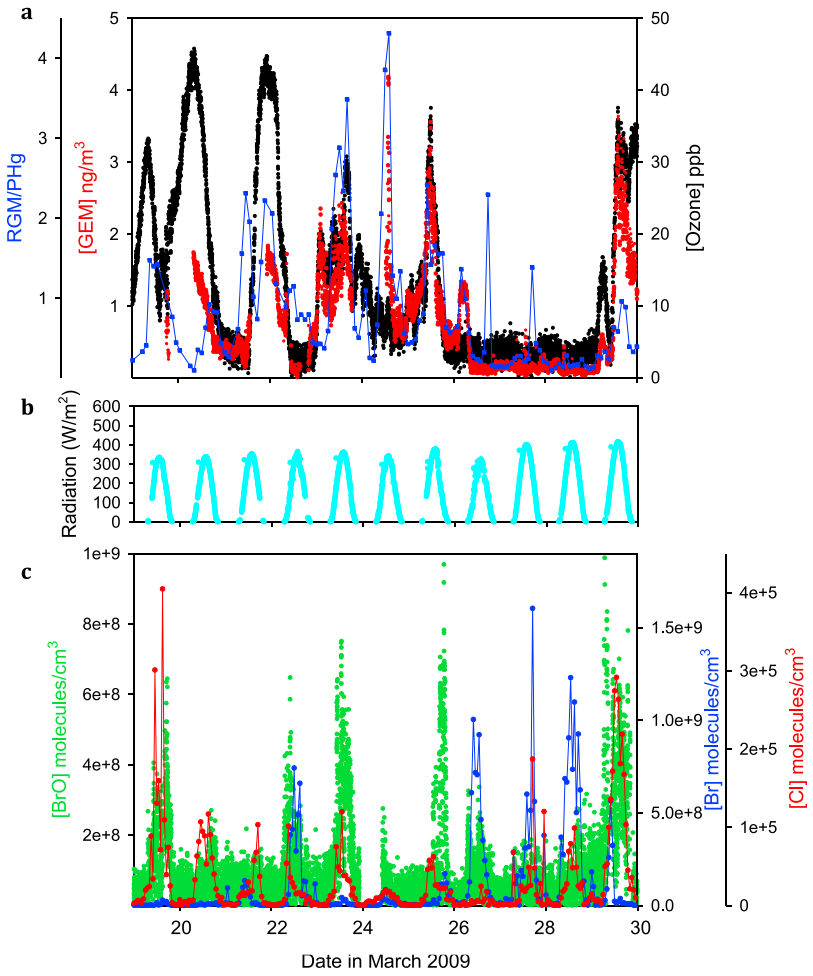

Figure 1. (a) Times series of ozone and GEM for the period 19–30 March 2009, including RGM/PHg ratio; (b) radiation; (c) calculated [Cl], [Br], and observed [BrO].

toluene, the C_8-aromatic VOCs), oxygenated VOCs (OVOCs; acetaldehyde (CH_3CHO), methanol (CH_3OH), ethanol (C_2H_5OH), acetone (CH_3COCH_3), propanal (C_3H_6O), butanal (C_4H_8O), methyl ethyl ketone (MEK; $C_2H_5COCH_3$) methyl *tert*-butyl ether (MTBE; $C(CH_3)_3OCH_3$)), halogenated VOCs (chloromethane (CH_3Cl), bromomethane (CH_3Br), dichloromethane (CH_2Cl_2), chloroform ($CHCl_3$), tetrachloromethane (CCl_4)), acetonitrile (CH_3CN) and dimethylsulfide (DMS; CH_3SCH_3).

[20] In addition, whole air samples were collected in electropolished stainless steel canisters through the same manifold used by TOGA. The canisters were typically pressurized to 2000 hPa. Approximately three samples were collected each day. The sample integration period was approximately 40 s. After collection, the canisters were transported back to NCAR or the University of New Hampshire and analyzed for more than 50 trace gases. At NCAR a subset of the samples were analyzed for NMHCs, selected halocarbons, and selected OVOCs. At the University of New Hampshire all samples were analyzed for NMHCs, halocarbons, DMS, alkyl nitrates, and selected OVOCs [*Russo et al.*, 2010]. The reported detection limits are 3 pptv for most NMHC and sub-pptv for halocarbons. The precision of the C_2–C_4 NMHC analysis was ±3% when compared to NIST standards during the Nonmethane Hydrocarbon Intercomparison Experiment (NOMHICE) [*Apel et al.*, 1994, 1999].

3. Results

[21] In Barrow, Alaska, ozone concentrations began to exhibit depletion events in early February following polar sunrise. As the season progressed, stronger depletions with nearly complete destruction of ozone occurred through late March and April, and ceased after the onset of melt [*Knepp et al.*, 2010]. Similar to observations at other Arctic locations, atmospheric mercury also exhibited depletion events during this time period in concert with ODEs. Figure 1a shows a portion of the time series profile of ozone and GEM measurements during the OASIS campaign. This time series covers background and fully depleted conditions, as well as periods of apparent GEM evasion from the tundra snowpack.

3.1. Steady State Calculations of Cl and Br Atom Concentrations

[22] While the aim of this study was to investigate the relative contribution of halogen radicals to the GEM depletions observed in Barrow, there is currently no suitable

analytical technique capable of directly determining chlorine or bromine atom concentrations in the ambient air. Therefore, we applied a steady state approximation (certainly valid for these very short-lived atoms) to calculate the concentrations of Cl and Br using the time-resolved data sets described above. [Cl] and [Br] were calculated using known source (numerator) and sink (denominator) terms according to equations (1) and (2).

$$[Cl]_{ss} = \frac{(2J[Cl_2] + J[BrCl] + J[ClO] + k[Cl_2][OH] + k[ClO][OH] + k[ClO][NO] + k[ClO][ClO])}{(k[HO_2] + k[O_3] + k[MEK] + k[CH_4] + k[C_2H_2] + k[C_2H_4] + k[C_2H_6] + k[C_3H_6] + k[C_3H_8] + k[iC_4H_{10}] + k[nC_4H_{10}] + k[HCHO] + k[CH_3CHO])} \quad (1)$$

$$[Br]_{ss} = \frac{(2J[Br_2] + J[BrCl] + J[BrO] + J[HOBr] + k[Br_2][OH] + k[BrO][NO] + k[BrO][ClO] + 2k[BrO][BrO] + k[BrO][OH])}{(k[HO_2] + k[O_3] + k[NO_2] + k[HCHO] + k[CH_3CHO] + k[C_2H_2] + k[C_2H_4] + k[C_3H_6])} \quad (2)$$

[23] Here, "J" represents the specific photodissociation rate coefficient for the species photolyzing at the appropriate time of day. The k in each case represents the second-order rate constant for the reaction producing or destroying the halogen atom. The self-reaction of ClO is estimated here to only regenerate 1 Cl atom based on the work of *Horowitz et al.* [1994], who found a 0.61 branching ratio for this product. The minority product is Cl_2 (0.39 branching ratio), however, Cl_2 is explicitly accounted for in our calculation from its measurement. An analogous situation exists for the BrO + ClO cross reaction, which only directly generates a Br radical as the major reaction pathway [*Friedl and Sander*, 1989], therefore, this reaction is not considered for Cl atom production. It should be noted that HOCl photolysis is not included because this compound was not measured during the campaign. We assume that [HOCl] is small for the purposes of this approximation; however, if [HOCl] is significant, we are likely underestimating [Cl].

[24] Alternatively, and as a means to assess uncertainties in the atom concentration estimates, Cl and Br atom concentrations can be calculated assuming a steady state on ClO and BrO, respectively, via equations (3) and (4).

$$[Cl]_{ss} = \frac{(J[ClO] + k[ClO][BrO] + k[ClO][OH] + k[ClO][HO_2] + k[ClO][NO] + k[ClO][NO_2] + 2k[ClO][ClO])}{k[O_3]} \quad (3)$$

$$[Br]_{ss} = \frac{(J[BrO] + k[BrO][NO] + k[BrO][NO_2] + k[BrO][ClO] + 2k[BrO][BrO] + k[BrO][HO_2] + k[BrO][OH])}{k[O_3]}. \quad (4)$$

[25] Comparisons of the results from the two methods for each halogen (denoted Br_{ss} versus BrO_{ss} and Cl_{ss} versus ClO_{ss}, respectively) yielded reasonably good agreement; however, the BrO_{ss} and ClO_{ss} methods yielded consistently higher halogen atom concentrations. Figure 2 illustrates the ratio of [Br] as calculated via the BrO_{ss} method and the Br_{ss} method, versus ambient ozone concentration. The ratio $[Br]_{BrO\text{-}ss}/[Br]_{Br\text{-}ss}$ averages 1.8 at ozone concentrations greater than 1 ppbv. Below 1 ppbv, this relationship degrades rapidly, possibly due to other, unknown mechanisms for BrO production (e.g., $Br_2 + O$). This reasonable agreement in [Br] between two mostly independent methods of calculation lends confidence to the estimations used in this analysis (for $[O_3] > 1$ ppbv).

[26] There is a significantly larger discrepancy in [Cl] between the two methods of calculation, on average by a factor of 5 (data not shown). Similar to the case for BrO_{ss}/Br_{ss}, at low ozone concentrations, the ClO_{ss}/Cl_{ss} drastically increases. However, the ClO data are much more limited; for this campaign, there is significantly more Cl_2 data than ClO data, and thus the Cl_{ss} method is preferred for this analysis. Note also that equations (1) and (2) are mostly dependent on measurement of stable (closed shell) species, while equations (3) and (4) rely more on measurements of radical species. We therefore use equations (1) and (2) for the following analysis of the GEM sinks. Since equation (2) yields significantly lower results than for equation (4), our results for the Cl atom contribution may be underestimated.

[27] Calculations were performed using equations (1) and (2) such that [Br] and [Cl] concentrations were generated hourly for the time period of 18 March through 5 April. Unless otherwise noted, rate constants were taken from the preferred values in the IUPAC Subcommittee for Gas Kinetic Data Evaluation [*Atkinson et al.*, 2004, and references therein], and are listed in Table 2. A temperature of 248 K was used to calculate all rate constants, which is consistent with average temperatures in Barrow during the month of March. Photolysis rate coefficients (J values) used here were calculated using a modified version of the Tropospheric Ultraviolet and Visible (TUV) radiation model [*Madronich and Flocke*, 1999] for the duration of the campaign based on in situ measurements of downwelling actinic flux. The charged-coupled device Actinic Flux Spectroradiometer (CAFS) [*Shetter and Müller*, 1999] measured spectrally resolved downwelling actinic flux at 0.1 Hz. The upwelling was estimated as a function of solar zenith angle using the

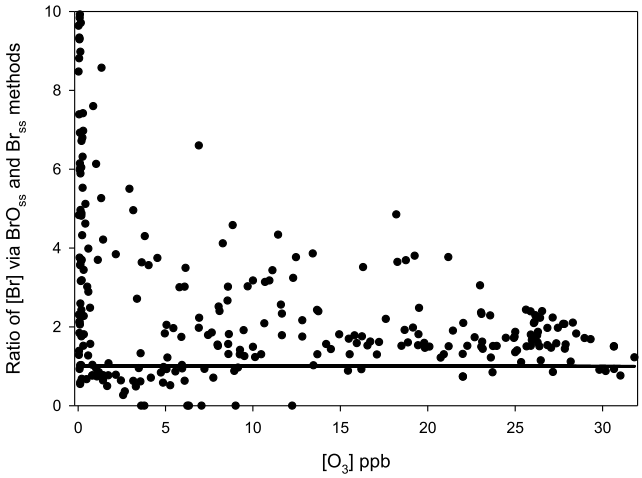

Figure 2. The ratio of [Br] calculated via equations (4) (BrO steady state method) and (2) (Br steady state method) versus ozone concentration. A 1:1 line for the bromine atom ratio is included.

TUV model under clear sky conditions. The sum of upwelling and downwelling actinic flux was used to calculate total photolysis frequencies.

[28] Short discontinuities in the various data sets were replaced with estimates interpolated based on concentrations immediately prior to and following the gap. Data gaps longer than half a day were left as breaks. Propagation of errors associated with both measurement uncertainties and rate constants, given the individual component variances, result in an overall average uncertainty for the steady state approximations of +38%/−33% for [Br] and +46%/−32% for [Cl] using equations (1) and (2).

[29] The resulting bromine and chlorine atom concentrations for the period of 20–29 March are plotted in Figure 1c, along with observed [BrO]. Surface downwelling irradiance is shown in Figure 1b as a reference to solar intensity to illustrate time of day. Br atom concentrations peaked at levels of 1.6×10^9 molecules/cm^3, while Cl atoms reached 4×10^5 molecules/cm^3. [Br] attained its highest levels when severe ozone depletion was observed (i.e., when the rate of Br + O_3 is small), most notably during the 3 day event that began on 26 March. Some peaks in RGM/PHg (Figure 1a) occurred during this period, which suggests possible reoxidation of GEM emitted from the surface snowpack, as peaks in RGM production are indicative of local chemistry [*Steen et al.*, 2011]. The Br and Cl concentrations calculated here are relatively large compared to those determined from VOC decays, possibly because they are calculated from near-surface layer data, while VOCs integrate the signal over their transport path, which includes a component aloft where halogen atom concentrations will be lower [*Tackett et al.*, 2007]. Interestingly, Br and Cl fluctuate independently of each other. Notably, the extended ODE of 26 March is characterized by relatively high [Br] and relatively low [Cl]. However, this switches with the return of ozone on 29 March to a condition of relatively higher chlorine activity. This may be due to the fact that Br will tend to vary inversely with O_3, which is often its dominant sink, while it appears that O_3 is required for Cl_2 production (Liao et al., manuscript in preparation, 2012). That chlorine and bromine do not vary together is an observation that has also been noted in studies by *Impey et al.* [1997b] and *Shepson et al.* [1996], and is discussed by Liao et al. (manuscript in preparation, 2012) in reference to the OASIS field study.

3.2. Contribution of Atmospheric Oxidants to GEM Depletion

[30] To evaluate the contribution of the halogen radicals, O_3, and OH to the oxidation of GEM, the relative rates of GEM depletion by each oxidant were calculated during periods when GEM exhibited an apparent first-order decay, potentially indicative of significant local chemistry, the rate of which can be compared with the calculated rate. While it is quite possible that any observed decay event results from transport of previously depleted air from upwind, it is useful to be able to compare the observed rate and the calculated potential oxidative chemical depletion rate, given the locally measured oxidant concentrations and rate constants. Five such events in late March were chosen for this analysis: 20, 22, 23, 24 and 25 March. The peak in GEM on 24 March was likely a result of reemission from the snowpack, therefore, we use only the data when GEM was below background values. Meteorological data indicate wind speeds less than

Table 2. Rate Constants Used in Equations (1)–(4)[a]

Reaction	k (cm^3 molecule^{-1} s^{-1} at 248 K)
Cl_2 + OH	2.9×10^{-14}
Cl + HO_2	4.2×10^{-11}
Cl + O_3	1.0×10^{-11}
Cl + MEK (methyl ethyl ketone)	4.2×10^{-11}
Cl + CH_4	4.5×10^{-14}
Cl + C_2H_2	2.5×10^{-10}
Cl + C_2H_4	1.0×10^{-9}
Cl + C_2H_6	5.6×10^{-11}
Cl + C_3H_6	2.7×10^{-10}
Cl + C_3H_8	1.4×10^{-10}
Cl + iC_4H_{10}	1.3×10^{-10}[b]
Cl + nC_4H_{10}	2.2×10^{-10}[c]
Cl + HCHO	7.1×10^{-11}
Cl + CH_3CHO	8.1×10^{-11}
ClO + OH	2.5×10^{-11}
ClO + NO	2.0×10^{-11}
ClO + ClO	2.9×10^{-15}
ClO + BrO	1.7×10^{-11}
ClO + HO_2	8.1×10^{-12}
ClO + NO_2	7.1×10^{-12}
Br_2 + OH	5.0×10^{-11}
Br + HO_2	1.3×10^{-12}
Br + O_3	6.8×10^{-13}
Br + NO_2	1.5×10^{-11}
Br + HCHO	7.4×10^{-13}
Br + CH_3CHO	2.8×10^{-12}
Br + C_2H_2	3.7×10^{-14}
Br + C_2H_4	1.3×10^{-13}
Br + C_3H_6	1.6×10^{-12}
BrO + NO	2.5×10^{-11}
BrO + ClO	1.6×10^{-11}
BrO + BrO	2.7×10^{-12}
BrO + OH	4.9×10^{-11}
BrO + NO_2	1.9×10^{-11}
BrO + HO_2	3.4×10^{-11}

[a]All rate constants are derived from recommended values in the IUPAC Subcommittee for Gas Kinetic Data Evaluation [*Atkinson et al.*, 2004] and calculated for 248 K unless otherwise specified.
[b]From *Hooshiyar and Niki* [1995] at 298 K.
[c]From *Tyndall et al.* [1997] at 298 K.

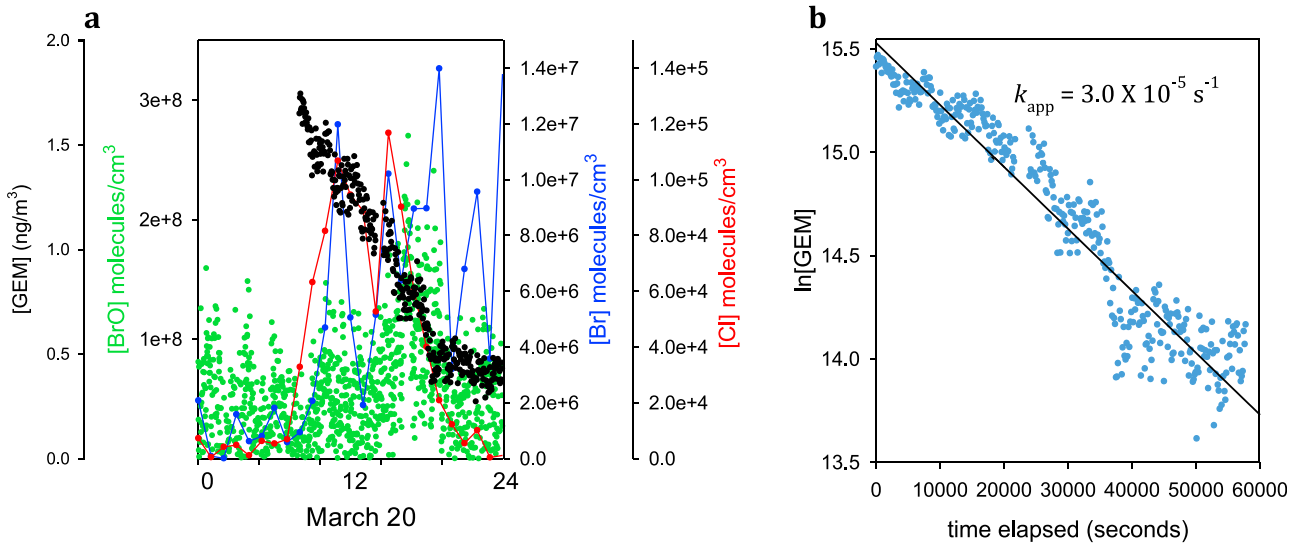

Figure 3. (a) GEM, BrO, and calculated Br and Cl for the example case of 20 March. (b) First-order rate plot of GEM decay for 20 March.

5 m/s or calm conditions for all five events (NOAA National Weather Service), increasing the likelihood that the event scale is local. Measurements of RGM and PHg for these periods (shown as the blue trace in Figure 1a) reveal a predominance of RGM over PHg, also consistent with the assumption of local chemistry. A greater relative concentration of PHg is expected in AMDEs of nonlocal origin [*Cobbett et al.*, 2007; *Lindberg et al.*, 2002; *Steen et al.*, 2011], because of its longer lifetime. An example of the depletion for 20 March is shown in Figure 3a, which also shows some of the important observed or calculated halogen radical concentrations.

[31] Each depletion event was plotted as ln([GEM]) versus the time elapsed (in seconds) from the start of the observed depletion. If we assume first-order conditions (i.e., the oxidant concentrations are constant), then the negative of the slope of the linear regression is taken as the apparent first-order decay rate constant, k_{app}. This k_{app} can then be compared to k_{calc}, which is ($k_{GEM+oxidant\ 1}$[oxidant 1] + $k_{GEM+oxidant\ 2}$[oxidant 2] + …). The apparent first-order decay for the example case of 20 March is illustrated in Figure 3b.

[32] To determine the potential contribution of each known oxidant to Hg° decay during a depletion event, the calculated first-order decay rate constant, k_{calc}, was determined as shown in equation (5) using the average oxidant concentration for the event, where each k represents the rate constant for the appropriate reaction of that oxidant with GEM.

$$k_{calc} = k[\mathrm{Br}] + k[\mathrm{Cl}] + k[\mathrm{BrO}] + k[\mathrm{ClO}] + k[\mathrm{OH}] + k[\mathrm{O_3}]. \quad (5)$$

[33] The rate constant for gas-phase Hg° reaction with Br, 6.1×10^{-13} cm^3 molecule^{-1} s^{-1}, was calculated for 248 K from *Donohoue et al.* [2006] using the reported Arrhenius expression. The Hg° + Cl rate constant, 1.0×10^{-12} cm^3 molecule^{-1} s^{-1}, was calculated from *Donohoue et al.* [2005]. While there is a large range in the reported rate constants between studies for the chlorine atom reaction (see Table 1 for a summary), we have chosen to use the Donohoue et al. values because this work was an absolute rate study performed in N_2 that demonstrated consistent results when performed with either Cl or Hg° in excess. Moreover, observational evidence suggests that O_2 may enhance the apparent rate constant through side reactions (perhaps ClO_2 + Hg° [*Donohoue et al.*, 2005; *Hynes et al.*, 2009]), thus, relative rate studies performed in air may not be appropriate for this particular reaction. The rate constant for O_3, 7.5×10^{-19} cm^3 molecule^{-1} s^{-1}, was taken from *Pal and Ariya* [2004b], and those for BrO and ClO were from *Spicer et al.* [2002]. The rate constant for Hg° reaction with OH, 8.7×10^{-14} cm^3 molecule^{-1} s^{-1}, was taken from *Sommar et al.* [2001]. We note that the rate constants for OH and O_3 should be taken as upper limits, given the computational results for HgO thermochemistry, discussed by *Hynes et al.* [2009]. The rate constants and their reported uncertainties are shown in Table 3. With the exception of Br and Cl, all rate constants used here were measured at room temperature. Atomic recombination reactions exhibit only very weak negative or no temperature dependence [*Ariya et al.*, 2002; *Goodsite et al.*, 2004], therefore, the rate constants used here are assumed to be valid in the low temperatures of the Arctic troposphere. The average concentrations for each oxidant for the period of decay for 20 March are also shown in Table 3, along with the resultant individual k[oxidant].

[34] The k_{calc} obtained from equation (5) results in the total GEM depletion rate constant that can be accounted for by known gas-phase chemical transformation pathways. The individual and cumulative contributions for the oxidants are shown in Figure 4, plotted as the apparent first-order decay rate constant versus the calculated first-order rate for oxidation by Br, Br + BrO, Br + BrO + Cl, Br + BrO + Cl + ClO, and all oxidants combined (i.e., including O_3 and OH). Both axes are shown on logarithmic scales. A 1:1 line is included for comparison. These values are also listed in Table 4.

[35] For two of the cases considered here (22 and 25 March), the observed decay rate is not inconsistent with local-scale chemical loss via reaction with bromine atoms

Table 3. Rate Constants Used for Calculations and Average Oxidant Concentrations for the Example Case of 20 March[a]

Oxidant (x)	Average Concentration (molecules cm^{-3})	$k_{(x + Hg)}$ (cm^3 $molecule^{-1}$ s^{-1})	$k_{calculated} = k$[oxidant] (s^{-1})
Br	$6.8\ (-2.3/+2.6) \times 10^6$	$6.1\ (\pm 2.2) \times 10^{-13}$[b]	$4.1\ (\pm 2.1) \times 10^{-6}$
Cl	$5.9\ (-2.7/+1.9) \times 10^4$	$1.0\ (\pm 0.7) \times 10^{-12}$[b]	$5.9\ (-5.0/+4.5) \times 10^{-8}$
BrO	$6.7\ (\pm 2.3) \times 10^7$	3.0×10^{-14}[c]	$2.0\ (\pm 0.7) \times 10^{-6}$
ClO	$8.1\ (\pm 1.2) \times 10^7$	3.6×10^{-17}[c]	$3.0\ (\pm 0.5) \times 10^{-9}$
O_3	$5.2\ (\pm 0.2) \times 10^{11}$	$7.5\ (\pm 0.9) \times 10^{-19}$[d]	$3.9\ (\pm 0.5) \times 10^{-7}$
OH	$7.8\ (\pm 3.6) \times 10^4$	$8.7\ (\pm 2.8) \times 10^{-14}$[e]	$6.8\ (\pm 3.8) \times 10^{-9}$

[a]Uncertainties in the rate constants are those reported in the respective references.
[b]Rate constants from *Donohoue et al.* [2005, 2006] calculated for 248 K.
[c]Rate constants from *Spicer et al.* [2002].
[d]Rate constant from *Pal and Ariya* [2004b].
[e]Rate constant from *Sommar et al.* [2001].

alone. However, in the remaining three cases, the calculated chemical loss rate is significantly less than the observed rate. This may be the case due to transport of an already-depleted air mass to the measurement site. That seems likely for a case such as 24 March, when k_{app} is ~9 times greater than k_{calc}. Interestingly, in four cases, BrO contributes a significant amount to the GEM decay. In no case studied here does Cl or ClO have a significant contribution to GEM depletion. This observation is especially interesting given the exceptionally high Cl_2 mole fractions observed in Barrow during this campaign, with some days reaching over 400 pptv, and Cl atom concentrations as high as 4×10^5 molecules/cm^3. It should be noted, however, that the Hg° + Cl rate constant used here is on the low end of all reported values, and it is possible that Cl could have a significant contribution if the rate constant were larger. For example, for 20 March, if the Cl atom rate constant were 1.0×10^{-11} cm^3 $molecule^{-1}$ s^{-1} [*Ariya et al.*, 2002], it would contribute 8.1% of the total k_{app}.

[36] Heterogeneous reactions are not considered here, but it is not expected that such reactions contribute significantly to GEM depletion. Elemental mercury is only sparingly soluble in water [*Shia et al.*, 1999] and aqueous phase reactions of Hg° with bromide and chloride are far too slow in comparison with gas-phase oxidation to be significant sinks [*Lin and Pehkonen*, 1998; *Wang and Pehkonen*, 2004]. Moreover, the low Henry's Law equilibrium constant for Hg°, 0.13 M/atm, results in a very small fraction of Hg° present in the aqueous phase. However, experimental evidence demonstrates that surface interactions can enhance reaction rate constants over that of pure gas phase, most notably for reactions of OH and O_3, wherein surfaces can stabilize the reaction intermediates. This would imply that GEM oxidation in the real atmosphere may occur more rapidly than suggested by gas-phase laboratory experiments [*Subir et al.*, 2011]. *Hedgecock et al.* [2005] included heterogeneous chemistry on both maritime and continental cloud droplets in a modeling study, and found that aqueous phase oxidation could account for 2–30% of GEM oxidation. Due to the low OH mole fractions in the Arctic, and the much lower abundance of cloud droplets as compared to the mid-latitude MBL, it is likely that the aqueous phase does not contribute highly to oxidation in the Arctic.

[37] Since mixing and dilution of air masses should decrease the apparent rate of decay, any statistically significant differences between the observed and calculated rates of depletion can only arise from two possibilities: (1) depletion occurred upwind, followed by transport of the depleted air to the measurement site, and/or (2) we are missing a GEM sink. Although it is clear that some local chemistry was occurring for these events, given the radical concentrations, the first explanation seems more likely, in part because we have considered most known atmospheric oxidants. A faster apparent time scale can thus occur if the depleted region is well defined at the edges, and that air mass transits the measurement site. We note that the radical concentrations that apply to the upwind depletion of Hg° may be significantly different from those calculated for the measurement site at Barrow. This relates to the distinctly different time scales for the lifetime of the radical precursors (e.g., Br_2 and Cl_2) and the time scale for mercury depletion. On average, the latter is 5 h as measured at Barrow. For a 5 m/s wind speed, this corresponds to a transport distance of 90 km. Since all of the back trajectories shown in Figure 5 extend out over the sea ice, it is quite possible that due to the higher surface salinity on sea ice, the actual atmospheric surface layer halogen concentrations where some of the depletion is occurring are higher than operative at Barrow, and thus we underestimate the absolute atom concentrations. This is supported by the fact that periods of exceptionally high Cl_2 have similar back trajectories over the sea ice [*Draxler and Rolph*, 2012; *Rolph*, 2012], similar to that shown as an example in Figure 5.

[38] From the local-scale oxidant concentration measurements, we can determine the fractional contribution of each

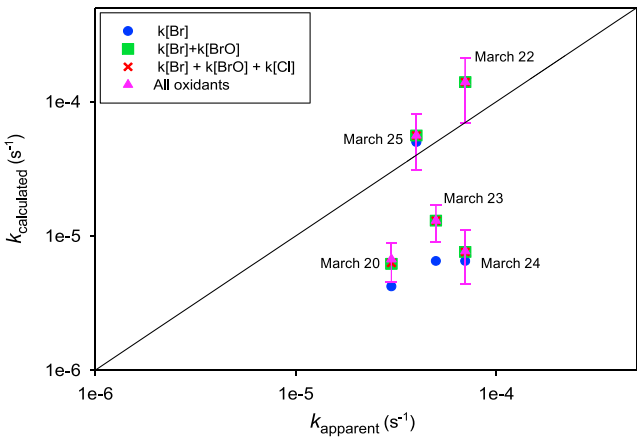

Figure 4. Cumulative contribution of known oxidants to GEM decay. A 1:1 line is included for comparison.

Table 4. Cumulative Oxidant Contributions for All Five Events (s^{-1}) in Comparison With $k_{apparent}$

Day in March	k[Br]	k[Br] + k[BrO]	k[Br] + k[BrO] + k[Cl]	k[Br] + k[BrO] + k[Cl] + k[ClO]	k[Br] + k[BrO] + k[Cl] + k[ClO] + k[O_3] + k[OH]	$k_{apparent}$
20	4.2×10^{-6}	6.2×10^{-6}	6.3×10^{-6}	6.3×10^{-6}	$6.7\ (+2.3/-2.3) \times 10^{-6}$	3×10^{-5}
22	1.4×10^{-4}	1.4×10^{-4}	1.4×10^{-4}	1.4×10^{-4}	$1.4\ (\pm 0.7) \times 10^{-4}$	7×10^{-5}
23	6.5×10^{-6}	1.3×10^{-5}	1.3×10^{-5}	1.3×10^{-5}	$1.3\ (\pm 0.4) \times 10^{-5}$	5×10^{-5}
24	6.5×10^{-6}	7.6×10^{-6}	7.6×10^{-6}	7.6×10^{-6}	$7.7\ (+3.4/-3.4) \times 10^{-6}$	7×10^{-5}
25	5.0×10^{-5}	5.6×10^{-5}	5.6×10^{-5}	5.6×10^{-5}	$5.6\ (+2.6/-2.4) \times 10^{-5}$	4×10^{-5}

oxidant to the total calculated decay. The results are shown in Figure 6, in the form of bar graphs constructed from the individual k[oxidant] values for Br, Cl, BrO, ClO, O_3 and OH, relative to k_{calc}. The uncertainties in the fractional contributions are shown as error bars representing the possible range of percent contribution for each oxidant. The uncertainties reported here are based on the reported uncertainties in the rate coefficients used and propagated uncertainties in the steady state Br and Cl atom concentrations. Therefore, it is likely that these values underestimate the true uncertainties since they do not include uncertainties resulting from discrepancies in the [Br] and [Cl] estimation methods and given the range of reported rate constants in the literature (Table 1).

[39] Figure 6 shows that of the total calculated decay, Br is the primary halogen radical driving the mercury loss for all events studied, consistent with the current hypotheses regarding AMDEs [*Brooks et al.*, 2006; *Calvert and Lindberg*, 2003; *Skov et al.*, 2004]. Though BrO does not dominate for any of the events, there is a significant contribution by BrO for the event on 23 March, with a smaller, though still significant, BrO contribution for 20, 24 and 25 March. This observation, and the relationship between Br and BrO, can help explain the temporal and spatial correlations sometimes seen between satellite BrO enhancements and ground level mercury depletion events [*Lindberg et al.*, 2002; *Lu et al.*, 2001]. Despite the high levels of Cl_2 observed during this time, Cl atoms did not contribute significantly to any of the events studied. O_3 also did not have a significant contribution due to the very slow rate constant, though there was a measurable contribution when ozone levels were higher. These days also correspond to days with higher BrO contribution, as would be expected since BrO is a product of Br reaction with ozone. Due to the very slow reaction rate constants for the Hg° + ClO and Hg° + OH, these oxidation pathways did not contribute significantly to any of the studied events. We note that a small or perhaps zero contribution from OH and O_3 reaction with GEM is expected from the discussion in the *Hynes et al.* [2009] work.

[40] As mentioned previously, the two different methods for calculating [Br] and [Cl] (i.e., Br_{ss} versus BrO_{ss} and Cl_{ss} versus ClO_{ss}) result in estimations for the atom concentrations that differ by a factor of 1.8 and 5, respectively. In order to

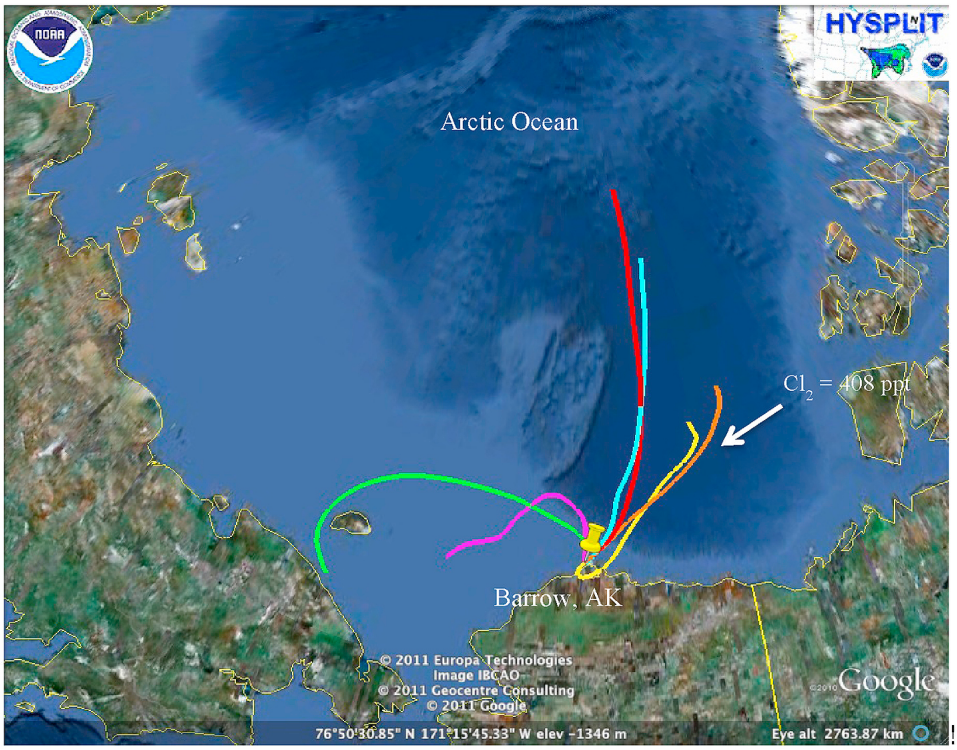

Figure 5. Shown are 48 h back trajectories for the five events studied: 20 March (yellow), 22 March (pink), 23 March (red), 24 March (cyan), and 25 March (green), with a representative day with very high Cl_2, 19 March, shown in orange.

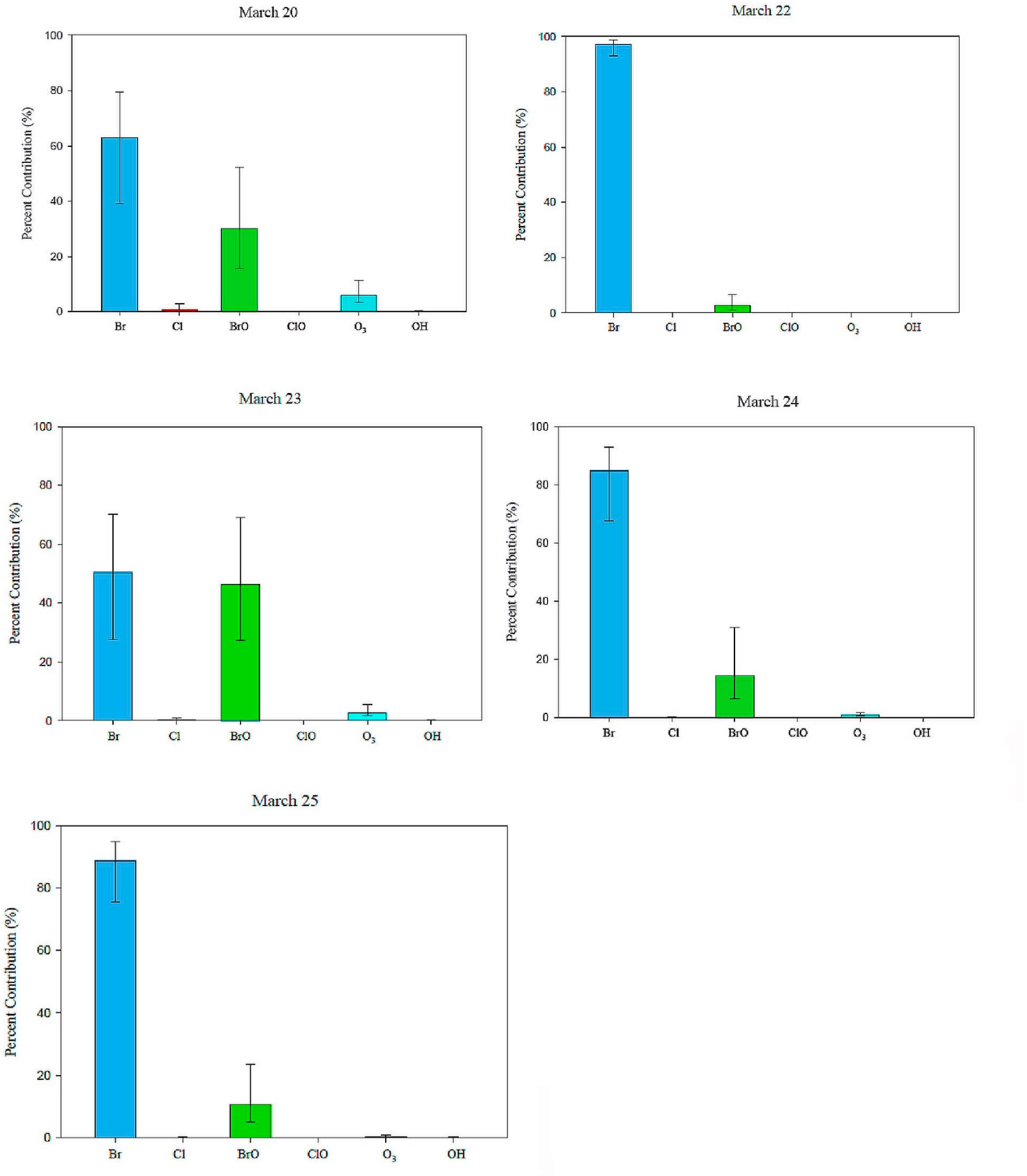

Figure 6. Bar graphs illustrating the percent contribution of the known gas-phase oxidation pathways to the depletion for which we can account. Error bars represent the high and low bounds as calculated from propagation of uncertainties associated with the oxidant concentrations and rate constants used.

determine whether this discrepancy would have any impact on the percent contribution results, the events for 20 and 22 March were recalculated using 5 times higher Cl atom concentrations. The date 22 March is a highly Br-dominant event, and using a higher [Cl] has no effect on the percent contribution calculated for Br. The date 20 March has a measurable Cl-atom contribution, and in this case, increasing [Cl] by a factor of five increases the Cl contribution from 0.9% to 4.3%, and decreases the Br contribution from 63% to 60%. In either case, the conclusion that Br is the dominant oxidizer of GEM for these events is not changed.

[41] A much more significant source of error for this analysis is the wide range in reported rate constants for the Cl + GEM reaction, from 1.0×10^{-12} to 6.4×10^{-11} cm^3 $molecule^{-1}$ s^{-1}. We have chosen to use the Arrhenius expression for k_3 from *Donohoue et al.* [2005], which is the lowest of all reported values. We believe this value to be the most reliable because it was an absolute rate study performed in N_2 bath gas, and consistent results were obtained with either Cl or Hg° in excess. The authors report a fourfold increase in the apparent rate constant when performed in air, which they speculate to result from secondary reactions between Hg° and either ClO or ClO_2. *Spicer et al.* [2002] measured a very small rate constant for Hg° + ClO, 3.6×10^{-17} cm^3 $molecule^{-1}$ s^{-1}, and thus it is not likely that ClO is causing the observed enhancement. Because Hg° + Cl is a third-order reaction, it is possible that ClO_2 reaction could be a more efficient pathway to form HgCl because it carries with it its own third body in O_2 [*Hynes et al.*, 2009]. In the relative rate studies performed by *Ariya et al.* [2002] the authors found inconsistent results depending on the reference compound used, and also observed nonlinearity in the relative rate plots, implying the possible effects of secondary chemistry. Based on these observations, relative rate studies performed in air are likely not appropriate for this particular reaction.

[42] The fourfold enhancement of the apparent Hg° + Cl reaction observed by *Donohoue et al.* [2005] in the presence of O_2 still does not account for the approximately 64-fold difference in the rate constant reported by *Spicer et al.* [2002]. The range in the reported rate constants is significant and it would have a dramatic impact on the results of this work if the larger values applied. For example, if the event on 20 March is recalculated using a rate constant of 6.4×10^{-11} cm^3 $molecule^{-1}$ s^{-1}, the contribution of Cl atoms to GEM decay becomes 45%, and Br becomes 40%. In this case, Cl would be the dominant oxidizer of GEM. While, as we have stated, there are good reasons for assuming that the *Donohoue et al.* [2005] values for k_3 are valid, it is apparent that more laboratory studies on gas-phase Hg° reactions would be helpful to better constrain these rate constants.

[43] The contribution of the halogen radicals to AMDEs is dependent on both their concentrations and reaction kinetics. Because there is no method for measuring Br or Cl directly, time-integrated estimates have been performed in previous studies using observed hydrocarbon decays. Using time-integrated [Br] and [Cl] derived from hydrocarbon decay methods of 1×10^7 and 1×10^4 molecules/cm^3, respectively, as has been done in previous studies [*Ariya et al.*, 2002, 2004; *Goodsite et al.*, 2004; *Skov et al.*, 2004], bromine-induced oxidation will always dominate mercury depletions. However, by examining the decay of GEM on a case-by-case basis, for conditions at the surface where most of the chemistry is likely occurring, it can be shown that as the relative concentrations of Br, Cl, and BrO fluctuate, and so too does their contribution to GEM oxidation. Though Cl itself does not display a significant direct contribution to GEM depletion based on our calculations (and chosen rate constants), it could be possible that the reaction of ClO_2 (formed by Cl + O_2) with Hg° may be a significant Hg° sink, thereby making Cl atoms indirectly important for AMDEs. Laboratory studies are needed to confirm this hypothesis. Note that while the hydrocarbon decay method explicitly integrates over a time scale corresponding to the lifetime of the VOCs, and thus potentially large spatial scales (including in the vertical direction), the halogen chemistry occurs in the very near surface environment [*Bottenheim et al.*, 2002; *Tackett et al.*, 2007]. *Tackett et al.* [2007] showed that chlorine chemistry and both ODEs (i.e., bromine chemistry) and AMDEs can occur in a shallow layer (~0–250 m) near the surface. This is also discussed by *Frieß et al.* [2011].

[44] The relative concentration of the halogen radicals appears to vary significantly, depending on [O_3]. When ozone is present, [BrO] is typically much greater than [Br], whereas during near-complete ozone depletion events, the ratio is shifted toward [Br] due to the removal of this major bromine atom sink. Indeed, there are cases when [Br] approaches 50 pptv, which is on the high end of all reported [BrO] measurements. Cl_2 observations from the OASIS field study show that molecular chlorine, the primary precursor of Cl, is only observed significantly above its detection limit when both ozone and radiation are present (Liao et al., manuscript in preparation, 2012), an observation similarly made by *Impey et al.* [1999] at Alert, Canada. This is also reflected in the Br and Cl steady state concentrations as mentioned previously, and well illustrated by the period of 26–29 March (Figure 1c). This points to an important role for ozone in mediating both the activation of chlorine, and the relative activity of the halogen radicals in mercury (and ozone) depletions. At high O_3, BrO (and potentially Cl atoms or ClO_2) will be important, but as O_3 concentrations deplete, the role of Br atoms will likely dominate. On the other hand, when O_3 is depleted, GEM is also typically nearly completely removed. Though ClO is also formed at high O_3, this is not a significant sink for GEM. Large Br atom concentrations calculated very late in an ODE/AMDE, i.e., when O_3 and GEM are effectively removed, will be the dominant oxidation pathway for GEM that is photochemically reemitted from the surface.

4. Discussion

[45] The results of this study imply that, in the polar regions, RGM will be composed of mostly Hg-Br compounds, though Hg-Cl compounds are possible. Because it is highly favorable for mercury to bind an additional atom in a two-step sequence, likely candidates for RGM would be $HgBr_2$, $HgCl_2$, HgBrO/OHgBr, and/or HgBrCl. Coupling of the initially formed Hg^I compound with a second ligand occurs in competition with thermal dissociation in a highly temperature-dependent manner. The cold temperatures of the Arctic can stabilize the initial Hg^I compound such that generation of the Hg^{II} product is more favorable than in the warmer temperatures of midlatitude regions. Product studies by *Ariya et al.* [2002] confirmed the formation of $HgBr_2$ and $HgCl_2$ upon reaction with only Br and only Cl atoms, respectively. However, in the atmosphere where numerous different species are present, it is likely that a significant portion of the RGM will be composed of Hg bound to two different atoms.

[46] *Calvert and Lindberg* [2004] suggested major RGM components to be OHgBr, BrHgOBr and HOHgBr based on a modeling study simulating conditions in Barrow. Though direct OH oxidation of GEM is not expected to be significant due to the low rate of reaction of OH with gas-phase Hg^o, and

very rapid dissociation of Hg-OH [*Goodsite et al.*, 2004], coupling of HgBr to OH is thought to be likely because of the similar bond strengths for BrHg-Br and BrHg-OH. However, the concentration of OH in the Arctic is generally quite low, 10^4–10^6 molecules/cm^3 based on measurements from OASIS, making it similar to the calculated levels of [Cl] and significantly less than [Br]. However, the Calvert and Lindberg study used only BrCl, at half the concentration of Br_2, as the chlorine atom source, and did not consider Cl_2. CIMS measurements of Cl_2 during OASIS indicate that molecular chlorine is much more prevalent than previously thought, and thus it is possible that more chlorinated-RGM products would be present in Barrow. An updated modeling study including a Cl_2 flux would be useful for investigating this situation.

[47] The presence of reactive iodine species (IO_x) has not been unambiguously detected in the High Arctic above instrumental detection limits; however, iodine-containing compounds have been observed in many coastal and lower-latitude locations [*Alicke et al.*, 1999; *Stutz et al.*, 1999], and it is speculated that they could potentially influence mercury oxidation. The only known experimental study of gaseous Hg° reaction with iodine [*Raofie et al.*, 2008] determined a rate constant for the Hg° + I_2 reaction of $\leq 1.27\ (\pm 0.58) \times 10^{-19}$ cm^3 molecule^{-1} s^{-1}, suggesting reaction with molecular iodine is too slow for rapid depletion of GEM. The same study determined the product of Hg° reaction with iodine atoms to be HgI_2, and that of Hg° reaction with IO to be HgIO/HgOI, however, the kinetics of these reactions were not determined. *Goodsite et al.* [2004] used Rice-Ramsperger-Kassel-Marcus (RRKM) theory to calculate a rate constant for the recombination of Hg and I and determined that it was 3–4 times slower than the recombination of Hg and Br. Thus, direct oxidation of mercury by iodine atoms is unlikely to be significant, with the possible exception of iodine-rich coastal locations with large algal populations [*Saiz-Lopez et al.*, 2007]. However, iodine can enhance radical concentrations in the polar atmosphere through the very fast cross reactions of IO + BrO and IO + ClO [*Platt and Hönninger*, 2003]. Moreover, the bond strength of BrHg-I is very close to that of BrHg-Br, and the product HgBrI is extremely stable [*Goodsite et al.*, 2004]. Due to the expected low concentrations of reactive iodine species in the Arctic, *Calvert and Lindberg* [2004] suggest that iodine-containing RGM species should be only minor products, and likely in the form of HgBrI, IOHgBr, or HgICl. IO has recently been detected in Antarctica at concentrations up to 20–50 ppt [*Frieß et al.*, 2010; *Saiz-Lopez et al.*, 2007]. The sub-Arctic location of Kuujjuarapik (Canada) has also been found to have IO present up to 3.4 pptv [*Mahajan et al.*, 2010]. These locations are known to experience ozone and mercury depletion events [*Dommergue et al.*, 2010; *Steffen et al.*, 2005], and the iodine levels present could lead to greater formation of iodinated RGM compounds there. Based on the current lack of successful IO measurements in the High Arctic (limit of detection for LP-DOAS is 1–2 pptv [*Saiz-Lopez et al.*, 2007]), it is not expected that iodine compounds would represent a significant fraction of RGM in this region.

[48] From the complex nature of RGM, it is crucial to develop methods to identify these compounds. However, given gas phase concentrations on the order of 100 ppqv for the total RGM, which is likely made up of multiple different reactive species, this is a very formidable challenge. Because the bond strengths and stabilities of various Hg^{II} compounds can be quite different, their fate in the environment could also vary. Highly soluble Hg^{II} compounds are readily scavenged to snow and ice surfaces and particles where they can be chemically transformed further. Mercury concentrations have been measured to reach 90–820 ng/L in surface snow during AMDEs [*Douglas et al.*, 2005; *Lindberg et al.*, 2002]. A portion of deposited RGM is photoreduced back to elemental mercury and reemitted to the atmosphere, though estimates of the fraction of mercury that is reemitted varies from slightly over half to upward of 92% [*Brooks et al.*, 2006; *Lalonde et al.*, 2002; *Lindberg et al.*, 2002; *Poulain et al.*, 2004]. Despite the large range, it is generally agreed that the Arctic acts as a net sink for atmospheric mercury [*Ariya et al.*, 2004; *Hirdman et al.*, 2009; *Skov et al.*, 2004], and that some of the deposited Hg^{II} is incorporated in the ecosystem during snowmelt in bioavailable forms [*Lindberg et al.*, 2002]. Understanding the cycling and fate of mercury compounds in the environment, and their potential effects on the people and wildlife of the region, will require further investigation into the chemical composition of these species.

5. Conclusion

[49] Using in situ field measurements from Barrow, Alaska, this work has investigated the relative contribution of reactive halogen radicals to the rapid oxidation of atmospheric mercury during polar spring. Br is the dominant oxidation pathway for all events studied here, with significant contributions from BrO. No significant contribution was found from Cl atoms directly, though it is possible that Cl may have an indirect effect through ClO_2. It is also possible that we have underestimated the importance of Cl in mercury depletions given the large range in reported rate constants. The contribution of individual oxidants is of course dependent on their relative concentrations, thus, it is likely that RGM products in Barrow are not only highly complex, but also variable depending on the dominant oxidation mechanism involved, and represent a mixture of Hg^{II} compounds. Both chemical and meteorological conditions are important mediators of the relative activities of the halogen radicals. When ozone is present, [BrO] > [Br], and [Cl] is relatively large, and thus they both contribute more to mercury depletion under those conditions. Interestingly, while O_3 is not itself an important GEM oxidant, its presence likely catalyzes the production of Cl (and possibly Br) atoms, and thus may have a significant indirect impact [*Oum et al.*, 1998a, 1998b; Liao et al., manuscript in preparation, 2012]. The independent behavior of Br and Cl suggests a different source or different activation mechanism is controlling these two species. The results of this study highlight the importance of halogen chemistry in general in chemical cycling in the polar regions. Identification of RGM compounds is absolutely crucial because their chemical composition is likely to influence their fate and/or bioavailability in the environment. It is also imperative that the rate constants for the gas-phase oxidation of Hg° by halogen radicals, especially Cl and ClO_2, continue to be studied, including at temperatures relevant to the polar regions, since these values represent a large uncertainty in our knowledge of GEM

depletions. This work demonstrates through quantitative analysis that bromine chemistry is likely controlling AMDEs in the polar regions, corroborating current hypotheses. However, there is also a potentially important role of chlorine atoms in the oxidation of not only VOCs, but also GEM and ozone, thus, the mechanism for production of Cl_2 also needs to be determined.

[50] **Acknowledgments.** This work was funded by the National Science Foundation, grant ARC-0732556. The authors wish to thank the organizers of the OASIS 2009 field campaign, the Barrow Arctic Science Consortium for logistical support (especially the illustrious Lewis Brower), and the numerous researchers that collaborated in OASIS. A.S. and J.B. wish to thank the Canadian IPY Research Program for funding. We also thank Tony Hynes for a careful review of the manuscript and helpful suggestions for improving this work.

References

Alicke, B., K. Hebestreit, J. Stutz, and U. Platt (1999), Iodine oxide in the marine boundary layer, *Nature*, *397*, 572–573, doi:10.1038/17508.

Apel, E., J. Calvert, and F. Fehsenfeld (1994), The Nonmethane Hydrocarbon Intercomparison Experiment (NOMHICE): Tasks 1 and 2, *J. Geophys. Res.*, *99*, 16,651–16,664, doi:10.1029/94JD00086.

Apel, E., J. Calvert, T. Gilpin, F. Fehsenfeld, D. Parrish, and W. Lonneman (1999), The Nonmethane Hydrocarbon Intercomparison Experiment (NOMHICE): Task 3, *J. Geophys. Res.*, *104*, 26,069–26,086, doi:10.1029/1999JD900793.

Apel, E., L. Emmons, T. Karl, F. Flocke, A. Hills, S. Madronich, J. Lee-Taylor, A. Fried, P. Weibring, and J. Walega (2010), Chemical evolution of volatile organic compounds in the outflow of the Mexico City metropolitan area, *Atmos. Chem. Phys.*, *10*, 2353–2375, doi:10.5194/acp-10-2353-2010.

Arctic Monitoring and Assessment Programme (AMAP) (2011), *Arctic Monitoring and Assessment Programme: Arctic Pollution 2011*, Oslo.

Ariya, P., B. Jobson, R. Sander, H. Niki, G. Harris, J. Hopper, and K. Anlauf (1998), Measurements of C_2–C_7 hydrocarbons during the Polar Sunrise Experiment 1994: Further evidence for halogen chemistry in the troposphere, *J. Geophys. Res.*, *103*, 13,169–13,180, doi:10.1029/98JD00284.

Ariya, P., A. Khalizov, and A. Gidas (2002), Reactions of gaseous mercury with atomic and molecular halogens: Kinetics, product studies, and atmospheric implications, *J. Phys. Chem. A*, *106*, 7310–7320, doi:10.1021/jp020719o.

Ariya, P., A. Dastoor, M. Amyot, W. Schroeder, L. Barrie, K. Anlauf, F. Raofie, A. Ryzhkov, D. Davignon, and J. Lalonde (2004), The Arctic: A sink for mercury, *Tellus, Ser. B*, *56*, 397–403, doi:10.1111/j.1600-0889.2004.00118.x.

Atkinson, R., D. L. Baulch, R. A. Cox, J. N. Crowley, R. F. Hampson, R. G. Hynes, M. E. Jenkin, M. J. Rossi, and J. Troe (2004), Evaluated kinetic and photochemical data for atmospheric chemistry: Volume I—Gas phase reactions of O_x, HO_x, NO_x and SO_x species, *Atmos. Chem. Phys.*, *4*, 1461–1738, doi:10.5194/acp-4-1461-2004.

Balabanov, N., and K. Peterson (2003), Mercury and reactive halogens: The thermochemistry of Hg+{Cl_2, Br_2, BrCl, ClO, and BrO}, *J. Phys. Chem. A*, *107*, 7465–7470, doi:10.1021/jp035547p.

Bottenheim, J., J. D. Fuentes, D. W. Tarasick, and K. G. Anlauf (2002), Ozone in the Arctic lower troposphere during winter and spring 2000 (ALERT2000), *Atmos. Environ.*, *36*, 2535–2544, doi:10.1016/S1352-2310(02)00121-8.

Boudries, H., and J. Bottenheim (2000), Cl and Br atom concentrations during a surface boundary layer ozone depletion event in the Canadian high Arctic, *Geophys. Res. Lett.*, *27*, 517–520, doi:10.1029/1999GL011025.

Brooks, S., A. Saiz-Lopez, H. Skov, S. Lindberg, J. Plane, and M. Goodsite (2006), The mass balance of mercury in the springtime arctic environment, *Geophys. Res. Lett.*, *33*, L13812, doi:10.1029/2005GL025525.

Calvert, J., and S. Lindberg (2003), A modeling study of the mechanism of the halogen-ozone-mercury homogeneous reactions in the troposphere during the polar spring, *Atmos. Environ.*, *37*, 4467–4481, doi:10.1016/j.atmosenv.2003.07.001.

Calvert, J., and S. Lindberg (2004), The potential influence of iodine-containing compounds on the chemistry of the troposphere in the polar spring: II. Mercury depletion, *Atmos. Environ.*, *38*, 5105–5116, doi:10.1016/j.atmosenv.2004.05.050.

Castro, L., A. Dommergue, C. Ferrari, and L. Maron (2009), A DFT study of the reactions of O_3 with Hg or Br, *Atmos. Environ.*, *43*, 5708–5711, doi:10.1016/j.atmosenv.2009.07.038.

Cobbett, F., A. Steffen, G. Lawson, and B. Van Heyst (2007), GEM fluxes and atmospheric mercury concentrations (GEM, RGM and HgP) in the Canadian Arctic at Alert, Nunavut, Canada (February–June 2005), *Atmos. Environ.*, *41*, 6527–6543, doi:10.1016/j.atmosenv.2007.04.033.

Dommergue, A., F. Sprovieri, N. Pirrone, R. Ebinghaus, S. Brooks, J. Courteaud, and C. Ferrari (2010), Overview of mercury measurements in the Antarctic troposphere, *Atmos. Chem. Phys.*, *10*, 3309–3319, doi:10.5194/acp-10-3309-2010.

Donohoue, D. L., D. Bauer, and A. J. Hynes (2005), Temperature and pressure dependent rate coefficients for the reaction of Hg with Cl and the reaction of Cl with Cl: A pulsed laser photolysis-pulsed laser induced fluorescence study, *J. Phys. Chem. A*, *109*, 7732–7741, doi:10.1021/jp0513541.

Donohoue, D. L., D. Bauer, B. Cossairt, and A. J. Hynes (2006), Temperature and pressure dependent rate coefficients for the reaction of Hg with Br and the reaction of Br with Br: A pulsed laser photolysis-pulsed laser induced fluorescence study, *J. Phys. Chem. A*, *110*, 6623–6632, doi:10.1021/jp054688j.

Douglas, T., M. Sturm, W. Simpson, S. Brooks, S. Lindberg, and D. Perovich (2005), Elevated mercury measured in snow and frost flowers near Arctic sea ice leads, *Geophys. Res. Lett.*, *32*, L04502, doi:10.1029/2004GL022132.

Draxler, R. R. and G. D. Rolph (2012), HYSPLIT (HYbrid Single-Particle Lagrangian Integrated Trajectory) Model, report, NOAA Air Resour. Lab., Silver Spring, Md. [Available via NOAA ARL READY Website (http://ready.arl.noaa.gov/HYSPLIT.php.]

Ferrari, C., C. Padova, X. Faïn, P. Gauchard, A. Dommergue, K. Aspmo, T. Berg, W. Cairns, C. Barbante, and P. Cescon (2008), Atmospheric mercury depletion event study in Ny-Alesund (Svalbard) in spring 2005: Deposition and transformation of Hg in surface snow during springtime, *Sci. Total Environ.*, *397*, 167–177, doi:10.1016/j.scitotenv.2008.01.064.

Foster, K., R. Plastridge, J. Bottenheim, P. Shepson, B. Finlayson-Pitts, and C. Spicer (2001), The role of Br_2 and BrCl in surface ozone destruction at polar sunrise, *Science*, *291*, 471–474, doi:10.1126/science.291.5503.471.

Friedl, R. R., and S. P. Sander (1989), Kinetics and product studies of the reaction chlorine monoxide + bromine monoxide using discharge-flow mass spectrometry, *J. Phys. Chem.*, *93*, 4756–4764, doi:10.1021/j100349a016.

Frieß, U., T. Deutschmann, B. Gilfedder, R. Weller, and U. Platt (2010), Iodine monoxide in the Antarctic snowpack, *Atmos. Chem. Phys.*, *10*, 2439–2456, doi:10.5194/acp-10-2439-2010.

Frieß, U., H. Sihler, R. Sander, D. Pöhler, S. Yilmaz, and U. Platt (2011), The vertical distribution of BrO and aerosols in the Arctic: Measurements by active and passive differential optical absorption spectroscopy, *J. Geophys. Res.*, *116*, D00R04, doi:10.1029/2011JD015938.

Goodsite, M., J. Plane, and H. Skov (2004), A theoretical study of the oxidation of Hg^0 to $HgBr_2$ in the troposphere, *Environ. Sci. Technol.*, *38*, 1772–1776, doi:10.1021/es034680s.

Hall, B. (1995), The gas phase oxidation of elemental mercury by ozone, *Water Air Soil Pollut.*, *80*, 301–315, doi:10.1007/BF01189680.

Hausmann, M., and U. Platt (1994), Spectroscopic measurement of bromine oxide and ozone in the high Arctic during Polar Sunrise Experiment 1992, *J. Geophys. Res.*, *99*, 25,399–25,413, doi:10.1029/94JD01314.

Hedgecock, I. M., G. A. Trufino, N. Pirrone, and F. Sprovieri (2005), Mercury chemistry in the MBL: Mediterranean case and sensitivity studies using the AMCOTS (Atmospheric Mercury Chemistry over the Sea) model, *Atmos. Environ.*, *39*, 7217–7230, doi:10.1016/j.atmosenv.2005.09.002.

Hirdman, D., K. Aspmo, J. Burkhart, S. Eckhardt, H. Sodemann, and A. Stohl (2009), Transport of mercury in the Arctic atmosphere: Evidence for a spring-time net sink and summer-time source, *Geophys. Res. Lett.*, *36*, L12814, doi:10.1029/2009GL038345.

Holmes, C., D. Jacob, and X. Yang (2006), Global lifetime of elemental mercury against oxidation by atomic bromine in the free troposphere, *Geophys. Res. Lett.*, *33*, L20808, doi:10.1029/2006GL027176.

Holmes, C., D. J. Jacob, E. S. Corbitt, J. Mao, X. Yang, R. Talbot, and F. Slemr (2010), Global atmospheric model for mercury including oxidation by bromine atoms, *Atmos. Chem. Phys.*, *10*, 12,037–12,057, doi:10.5194/acp-10-12037-2010.

Hooshiyar, P. A., and H. Niki (1995), Rate constants for the gas-phase reactions of Cl-atoms with C_2–C_8 alkanes at T = 296 ± 2 K, *Int. J. Chem. Kinet.*, *27*, 1197–1206, doi:10.1002/kin.550271206.

Horne, D., R. Gosavi, and O. Strausz (1968), Reactions of metal atoms: I. The combination of mercury and chlorine atoms and the dimerization of HgCl, *J. Chem. Phys.*, *48*, 4758–4764, doi:10.1063/1.1668058.

Horowitz, A., J. Crowley, and G. Moortgat (1994), Temperature dependence of the product branching ratios of the ClO self-reaction in oxygen, *J. Phys. Chem.*, *98*, 11,924–11,930, doi:10.1021/j100097a019.

Hynes, A. J., D. L. Donohoue, M. E. Goodsite, and I. M. Hedgecock (2009), Our current understanding of major chemical and physical processes affecting mercury dynamics in the atmosphere and at the air-water/terrestrial interfaces, in *Mercury Fate and Transport in the Global Atmosphere*, edited by N. Pirrone and R. Mason, pp. 427–457, Springer, New York, doi:10.1007/978-0-387-93958-2_14.

Impey, G., P. Shepson, D. Hastie, and L. Barrie (1997a), Measurement technique for the determination of photolyzable chlorine and bromine in the atmosphere, *J. Geophys. Res.*, *102*, 15,999–16,004, doi:10.1029/97JD00850.

Impey, G., P. Shepson, D. Hastie, L. Barrie, and K. Anlauf (1997b), Measurements of photolyzable chlorine and bromine during the Polar Sunrise Experiment 1995, *J. Geophys. Res.*, *102*, 16,005–16,010, doi:10.1029/97JD00851.

Impey, G., C. Mihele, K. Anlauf, L. Barrie, D. Hastie, and P. Shepson (1999), Measurements of photolyzable halogen compounds and bromine radicals during the Polar Sunrise Experiment 1997, *J. Atmos. Chem.*, *34*, 21–37, doi:10.1023/A:1006264912394.

Jobson, B., H. Niki, Y. Yokouchi, J. Bottenheim, F. Hopper, and R. Leaitch (1994), Measurements of C_2–C_6 hydrocarbons during the Polar Sunrise 1992 Experiment: Evidence for Cl atom and Br atom chemistry, *J. Geophys. Res.*, *99*, 25,355–25,368, doi:10.1029/94JD01243.

Kaleschke, L., A. Richter, J. Burrows, O. Afe, G. Heygster, J. Notholt, A. Rankin, H. Roscoe, J. Hollwedel, and T. Wagner (2004), Frost flowers on sea ice as a source of sea salt and their influence on tropospheric halogen chemistry, *Geophys. Res. Lett.*, *31*, L16114, doi:10.1029/2004GL020655.

Keil, A., and P. Shepson (2006), Chlorine and bromine atom ratios in the springtime Arctic troposphere as determined from measurements of halogenated volatile organic compounds, *J. Geophys. Res.*, *111*, D17303, doi:10.1029/2006JD007119.

Khalizov, A., B. Viswanathan, P. Larregaray, and P. Ariya (2003), A theoretical study on the reactions of Hg with halogens: Atmospheric implications, *J. Phys. Chem. A*, *107*, 6360–6365, doi:10.1021/jp0350722.

Knepp, T., J. Bottenheim, M. Carlsen, D. Carlson, D. Donohoue, G. Friederich, P. Matrai, S. Netcheva, D. Perovich, and R. Santini (2010), Development of an autonomous sea ice tethered buoy for the study of ocean-atmosphere-sea ice-snow pack interactions: The O-buoy, *Atmos. Meas. Tech.*, *3*, 249–261, doi:10.5194/amt-3-249-2010.

Lalonde, J., A. Poulain, and M. Amyot (2002), The role of mercury redox reactions in snow on snow-to-air mercury transfer, *Environ. Sci. Technol.*, *36*, 174–178, doi:10.1021/es010786g.

Liao, J., H. Sihler, L. Huey, J. Neuman, D. Tanner, U. Friess, U. Platt, F. Flocke, J. Orlando, and P. Shepson (2011), A comparison of Arctic BrO measurements by chemical ionization mass spectrometry and long path-differential optical absorption spectroscopy, *J. Geophys. Res.*, *116*, D00R02, doi:10.1029/2010JD014788.

Lin, C., and S. Pehkonen (1998), Oxidation of elemental mercury by aqueous chlorine (HOCl/OCl-): Implications for tropospheric mercury chemistry, *J. Geophys. Res.*, *103*, 28,093–28,102, doi:10.1029/98JD02304.

Lindberg, S., S. Brooks, C. Lin, K. Scott, M. Landis, R. Stevens, M. Goodsite, and A. Richter (2002), Dynamic oxidation of gaseous mercury in the Arctic troposphere at polar sunrise, *Environ. Sci. Technol.*, *36*, 1245–1256, doi:10.1021/es0111941.

Lu, J., W. Schroeder, L. Barrie, A. Steffen, H. Welch, K. Martin, L. Lockhart, R. Hunt, G. Boila, and A. Richter (2001), Magnification of atmospheric mercury deposition to polar regions in springtime: The link to tropospheric ozone depletion chemistry, *Geophys. Res. Lett.*, *28*, 3219–3222, doi:10.1029/2000GL012603.

Madronich, S., and S. Flocke (1999), The role of solar radiation in atmospheric chemistry, in *Handbook of Environmental Chemistry*, edited by P. Boule, pp. 1–26, Springer, Berlin.

Mahajan, A., M. Shaw, H. Oetjen, K. Hornsby, L. Carpenter, L. Kaleschke, X. Tian-Kunze, J. Lee, S. Moller, and P. Edwards (2010), Evidence of reactive iodine chemistry in the Arctic boundary layer, *J. Geophys. Res.*, *115*, D20303, doi:10.1029/2009JD013665.

Maron, L., A. Dommergue, C. Ferrari, M. Delacour Larose, and X. Faïn (2008), How elementary mercury reacts in the presence of halogen radicals and/or halogen anions: A DFT investigation, *Chemistry*, *14*, 8322–8329, doi:10.1002/chem.200800491.

Mauldin, R., III, D. Tanner, and F. Eisele (1999), Measurements of OH during PEM-Tropics A, *J. Geophys. Res.*, *104*, 5817–5827, doi:10.1029/98JD02305.

Montzka, S., C. Spivakovsky, J. Butler, J. Elkins, L. Lock, and D. Mondeel (2000), New observational constraints for atmospheric hydroxyl on global and hemispheric scales, *Science*, *288*, 500–503, doi:10.1126/science.288.5465.500.

Muthuramu, K., P. Shepson, J. Bottenheim, B. Jobson, H. Niki, and K. Anlauf (1994), Relationships between organic nitrates and surface ozone destruction during Polar Sunrise Experiment 1992, *J. Geophys. Res.*, *99*, 25,369–25,378, doi:10.1029/94JD01309.

Neuman, J., J. Nowak, L. Huey, J. Burkholder, J. Dibb, J. Holloway, J. Liao, J. Peischl, J. Roberts, and T. Ryerson (2010), Bromine measurements in ozone depleted air over the Arctic Ocean, *Atmos. Chem. Phys.*, *10*, 6503–6514, doi:10.5194/acp-10-6503-2010.

Nguyen, H., K. Kim, Z. Shon, and S. Hong (2009), A review of atmospheric mercury in the polar environment, *Crit. Rev. Environ. Sci. Technol.*, *39*, 552–584, doi:10.1080/10643380701764308.

Oum, K., M. Lakin, and B. Finlayson-Pitts (1998a), Bromine activation in the troposphere by the dark reaction of O_3 with seawater ice, *Geophys. Res. Lett.*, *25*, 3923–3926, doi:10.1029/1998GL900078.

Oum, K., M. Lakin, D. DeHaan, T. Brauers, and B. Finlayson-Pitts (1998b), Formation of molecular chlorine from the photolysis of ozone and aqueous sea-salt particles, *Science*, *279*, 74–76, doi:10.1126/science.279.5347.74.

Pal, B., and P. Ariya (2004a), Studies of ozone initiated reactions of gaseous mercury: Kinetics, product studies, and atmospheric implications, *Phys. Chem. Chem. Phys.*, *6*, 572–579, doi:10.1039/b311150d.

Pal, B., and P. Ariya (2004b), Gas-phase HO-initiated reactions of elemental mercury: Kinetics, product studies, and atmospheric implications, *Environ. Sci. Technol.*, *38*, 5555–5566, doi:10.1021/es0494353.

Perner, D., T. Arnold, J. Crowley, T. Klüpfel, M. Martinez, and R. Seuwen (1999), The measurement of active chlorine in the atmosphere by chemical amplification, *J. Atmos. Chem.*, *34*, 9–20, doi:10.1023/A:1006208828324.

Pirrone, N., et al. (2010), Global mercury emissions to the atmosphere from anthropogenic and natural sources, *Atmos. Chem. Phys.*, *10*, 5951–5964, doi:10.5194/acp-10-5951-2010.

Platt, U., and G. Hönninger (2003), The role of halogen species in the troposphere, *Chemosphere*, *52*, 325–338, doi:10.1016/S0045-6535(03)00216-9.

Pöhler, D., L. Vogel, U. Frieß, and U. Platt (2010), Observation of halogen species in the Amundsen Gulf, Arctic, by active long-path differential optical absorption spectroscopy, *Proc. Natl. Acad. Sci. U. S. A.*, *107*, 6582–6587, doi:10.1073/pnas.0912231107.

Poulain, A., J. Lalonde, M. Amyot, J. Shead, F. Raofie, and P. Ariya (2004), Redox transformations of mercury in an Arctic snowpack at springtime, *Atmos. Environ.*, *38*, 6763–6774, doi:10.1016/j.atmosenv.2004.09.013.

Pszenny, A., W. C. Keene, D. J. Jacob, S. Fan, J. R. Maben, M. P. Zetwo, M. Spring Young, and J. N. Galloway (1993), Evidence of inorganic chlorine gases other than hydrogen chloride in marine surface air, *Geophys. Res. Lett.*, *20*, 699–702, doi:10.1029/93GL00047.

Ramacher, B., J. Rudolph, and R. Koppmann (1999), Hydrocarbon measurements during tropospheric ozone depletion events: Evidence for halogen atom chemistry, *J. Geophys. Res.*, *104*, 3633–3653, doi:10.1029/1998JD100061.

Raofie, F., and P. Ariya (2003), Kinetics and products study of the reaction of BrO radicals with gaseous mercury, *J. Phys. IV*, *107*, 1119–1121, doi:10.1051/jp4:20030497.

Raofie, F., G. Snider, and P. A. Ariya (2008), Reaction of gaseous mercury with molecular iodine, atomic iodine, and iodine oxide radicals—Kinetics, product studies, and atmospheric implications, *Can. J. Chem.*, *86*, 811–820, doi:10.1139/v08-088.

Richter, A., F. Wittrock, M. Eisinger, and J. Burrows (1998), GOME observations of tropospheric BrO in Northern Hemispheric spring and summer 1997, *Geophys. Res. Lett.*, *25*, 2683–2686, doi:10.1029/98GL52016.

Ridley, B., F. Grahek, and J. Walega (1992), A small high-sensitivity, medium-response ozone detector suitable for measurements from light aircraft, *J. Atmos. Oceanic Technol.*, *9*, 142–148, doi:10.1175/1520-0426(1992)009<0142:ASHSMR>2.0.CO;2.

Rolph, G. D. (2012), Real-time Environmental Applications and Display sYstem (READY) Website, http://ready.arl.noaa.gov, NOAA Air Resour. Lab., Silver Spring, Md.

Rudolph, J., B. Fu, A. Thompson, K. Anlauf, and J. Bottenheim (1999), Halogen atom concentrations in the Arctic troposphere derived from hydrocarbon measurements: Impact on the budget of formaldehyde, *Geophys. Res. Lett.*, *26*, 2941–2944, doi:10.1029/1999GL010869.

Russo, R., Y. Zhou, M. White, H. Mao, R. Talbot, and B. Sive (2010), Multi-year (2004–2008) record of nonmethane hydrocarbons and halocarbons in New England: Seasonal variations and regional sources, *Atmos. Chem. Phys.*, *10*, 4909–4929, doi:10.5194/acp-10-4909-2010.

Saiz-Lopez, A., A. S. Mahajan, R. A. Salmon, S. J. B. Bauguitte, A. E. Jones, H. K. Roscoe, and J. Plane (2007), Boundary layer halogens in coastal Antarctica, *Science*, *317*, 348–351, doi:10.1126/science.1141408.

Schroeder, W., and J. Munthe (1998), Atmospheric mercury—An overview, *Atmos. Environ.*, *32*, 809–822, doi:10.1016/S1352-2310(97)00293-8.

Schroeder, W., K. Anlauf, L. Barrie, J. Lu, A. Steffen, D. Schneeberger, and T. Berg (1998), Arctic springtime depletion of mercury, *Nature*, *394*, 331–332, doi:10.1038/28530.

Shepson, P. B., A.-P. Sirju, J. F. Hopper, L. A. Barrie, V. Young, H. Niki, and H. Dryfhout (1996), Sources and sinks of carbonyl compounds in the Arctic Ocean boundary layer: Polar Ice Floe Experiment, *J. Geophys. Res.*, *101*, 21,081–21,089, doi:10.1029/96JD02032.

Shetter, R. E., and M. Müller (1999), Photolysis frequency measurements using actinic flux spectroradiometry during the PEM-Tropics mission: Instrumentation description and some results, *J. Geophys. Res.*, *104*, 5647–5661, doi:10.1029/98JD01381.

Shia, R., C. Seigneur, P. Pai, M. Ko, and N. Sze (1999), Global simulation of atmospheric mercury concentrations and deposition fluxes, *J. Geophys. Res.*, *104*, 23,747–23,760, doi:10.1029/1999JD900354.

Simpson, W., D. Carlson, G. Hönninger, T. Douglas, M. Sturm, D. Perovich, and U. Platt (2007a), First-year sea-ice contact predicts bromine monoxide (BrO) levels at Barrow, Alaska better than potential frost flower contact, *Atmos. Chem. Phys.*, *7*, 621–627, doi:10.5194/acp-7-621-2007.

Simpson, W., et al. (2007b), Halogens and their role in polar boundary-layer ozone depletion, *Atmos. Chem. Phys.*, *7*, 4375–4418, doi:10.5194/acp-7-4375-2007.

Skov, H., J. Christensen, M. Goodsite, N. Heidam, B. Jensen, P. Wåhlin, and G. Geernaert (2004), Fate of elemental mercury in the Arctic during atmospheric mercury depletion episodes and the load of atmospheric mercury to the Arctic, *Environ. Sci. Technol.*, *38*, 2373–2382, doi:10.1021/es030080h.

Slemr, F., E. G. Brunke, R. Ebinghaus, C. Temme, J. Munthe, I. Wängberg, W. Schroeder, A. Steffen, and T. Berg (2003), Worldwide trend of atmospheric mercury since 1977, *Geophys. Res. Lett.*, *30*(10), 1516, doi:10.1029/2003GL016954.

Sommar, J., K. Gårdfeldt, D. Strömberg, and X. Feng (2001), A kinetic study of the gas-phase reaction between the hydroxyl radical and atomic mercury, *Atmos. Environ.*, *35*, 3049–3054, doi:10.1016/S1352-2310(01)00108-X.

Spicer, C. W., J. Satola, A. A. Abbgy, R. A. Plastridge, and K. A. Cowen (2002), *Kinetics of Gas-Phase Elemental Mercury Reactions With Halogen Species, Ozone, and Nitrate Radical Under Atmospheric Conditions*, Fla. Dep. of Environ. Prot., Tallahassee.

Steen, A., T. Berg, A. Dastoor, D. Durnford, L. Hole, and K. Pfaffhuber (2011), Natural and anthropogenic atmospheric mercury in the European Arctic: A speciation study, *Atmos. Chem. Phys.*, *11*, 6273–6284, doi:10.5194/acp-11-6273-2011.

Steffen, A., W. Schroeder, R. Macdonald, L. Poissant, and A. Konoplev (2005), Mercury in the Arctic atmosphere: An analysis of eight years of measurements of GEM at Alert (Canada) and a comparison with observations at Amderma (Russia) and Kuujjuarapik (Canada), *Sci. Total Environ.*, *342*, 185–198, doi:10.1016/j.scitotenv.2004.12.048.

Steffen, A., et al. (2008), A synthesis of atmospheric mercury depletion event chemistry linking atmosphere, snow and water, *Atmos. Chem. Phys.*, *8*, 1445–1482, doi:10.5194/acp-8-1445-2008.

Stutz, J., K. Hebestreit, B. Alicke, and U. Platt (1999), Chemistry of halogen oxides in the troposphere: Comparison of model calculations with recent field data, *J. Atmos. Chem.*, *34*, 65–85, doi:10.1023/A:1006245802825.

Subir, M., P. A. Ariya, and A. P. Dastoor (2011), A review of uncertainties in atmospheric modeling of mercury chemistry I. Uncertainties in existing kinetic parameters—Fundamental limitations and the importance of heterogeneous chemistry, *Atmos. Environ.*, *45*, 5664–5676, doi:10.1016/j.atmosenv.2011.04.046.

Tackett, P., A. Cavender, A. Keil, P. Shepson, J. Bottenheim, S. Morin, J. Deary, A. Steffen, and C. Doerge (2007), A study of the vertical scale of halogen chemistry in the Arctic troposphere during Polar Sunrise at Barrow, Alaska, *J. Geophys. Res.*, *112*, D07306, doi:10.1029/2006JD007785.

Tokos, J., B. Hall, J. Calhoun, and E. Prestbo (1998), Homogeneous gas-phase reaction of Hg^0 with H_2O_2, O_3, CH_3I, and $(CH_3)_2S$: Implications for atmospheric Hg cycling, *Atmos. Environ.*, *32*, 823–827, doi:10.1016/S1352-2310(97)00171-4.

Tossell, J. (2003), Calculation of the energetics for oxidation of gas-phase elemental Hg by Br and BrO, *J. Phys. Chem. A*, *107*, 7804–7808, doi:10.1021/jp030390m.

Tuckermann, M., R. Ackermann, C. Gölz, H. Lorenzen-Schmidt, T. Senne, J. Stutz, B. Trost, W. Unold, and U. Platt (1997), DOAS-observation of halogen radical-catalysed arctic boundary layer ozone destruction during the ARCTOC-campaigns 1995 and 1996 in Ny-Ålesund, Spitsbergen, *Tellus, Ser. B*, *49*, 533–555, doi:10.1034/j.1600-0889.49.issue5.9.x.

Tyndall, G. S., J. J. Orlando, T. J. Wallington, M. Dill, and E. W. Kaiser (1997), Kinetics and mechanisms of the reactions of chlorine atoms with ethane, propane, and *n*-butane, *Int. J. Chem. Kinet.*, *29*, 43–55, doi:10.1002/(SICI)1097-4601(1997)29:1<43::AID-KIN6>3.0.CO;2-L.

Wang, Z., and S. Pehkonen (2004), Oxidation of elemental mercury by aqueous bromine: Atmospheric implications, *Atmos. Environ.*, *38*, 3675–3688, doi:10.1016/j.atmosenv.2004.02.059.

E. Apel, C. Cantrell, S. R. Hall, R. S. Hornbrook, D. J. Knapp, D. D. Montzka, and A. Weinheimer, National Center for Atmospheric Research, Boulder, CO 80307, USA.

J. W. Bottenheim and A. Steffen, Air Quality Research Division, Environment Canada, Toronto, ON M3H 5T4, Canada.

L. G. Huey and J. Liao, School of Earth and Atmospheric Sciences, Georgia Institute of Technology, Atlanta, GA 30332, USA.

P. B. Shepson and C. R. Stephens, Department of Chemistry, Purdue University, West Lafayette, IN 47907, USA. (pshepson@purdue.edu)

C. Sive, Department of Chemistry, Appalachian State University, Boone, NC 28608, USA.